NASA TN D-214

TECHNICAL NOTE
D-214

EXPERIMENTAL INVESTIGATION OF SPIN-UP FRICTION COEFFICIENTS ON CONCRETE AND NONSKID CARRIER-DECK SURFACES

By Walter B. Horne

Langley Research Center
Langley Field, Va.

NATIONAL AERONAUTICS AND SPACE ADMINISTRATION
WASHINGTON
April 1960

NATIONAL AERONAUTICS AND SPACE ADMINISTRATION

TECHNICAL NOTE D-214

EXPERIMENTAL INVESTIGATION OF SPIN-UP FRICTION COEFFICIENTS ON CONCRETE AND NONSKID CARRIER-DECK SURFACES

By Walter B. Horne

SUMMARY

A series of landing-impact tests was conducted with a carrier-type jet airplane main landing gear (dropping weight 6,630 pounds) to obtain data on tire spin-up friction coefficients at touchdown on both concrete and nonskid carrier-deck surfaces. Tire inflation pressures of 260, 320, and 400 pounds per square inch were used. The concrete-surface tests covered a forward velocity range from 76 to 97 knots and sinking speeds of 12 and 16 feet per second for a strut inclination of 2.5° forward. The nonskid carrier-deck tests ranged between 54 and 104 knots in forward speed and from 12 to 19 feet per second in sinking speed for strut inclinations of 2.5° forward and 5.1° rearward. Several impact and taxiing tests on a $1\frac{3}{8}$-inch-diameter arresting cable were also conducted.

Results indicated somewhat lower spin-up friction coefficients for the nonskid deck surface than for the concrete surface. The incremental landing-gear loads developed by impacting on and taxiing over the $1\frac{3}{8}$-inch arresting cable did not exceed about two-thirds of the static vertical load (6,630 pounds) on the landing gear for the conditions tested.

INTRODUCTION

One very important factor governing the design of aircraft for the landing condition is the magnitude and variation of the drag load developed during landing-gear-wheel spin-up immediately following initial touchdown. The importance of spin-up drag loads has been discussed in detail in reference 1. It is evident that the texture and physical properties of the landing surface could play an important part in this process. Past experimental research on the wheel spin-up

process, such as presented in references 1 to 4, has been limited to land runways and especially concrete runway surfaces. A large percentage of the landings for naval aircraft types, however, are made on aircraft-carrier deck surfaces, which for the later type carriers consists of a special nonskid coating that has been troweled over smooth steel decking. This nonskid coating is applied to the carrier decks primarily to increase traction for personnel and equipment during deck handling of aircraft while operating under adverse weather and sea conditions. In addition, carrier operational requirements and landing techniques are such that higher tire-inflation pressures and much higher sinking speeds are usually encountered in carrier landings than for equivalent land runway landings.

Tests were conducted at the Langley landing-loads track to extend the range of controlled test data on spin-up drag loads to include the regime of carrier experience in both tire-inflation pressure and sinking speed for both concrete and nonskid carrier deck surfaces. The purpose of this paper is to present the results of these tests which show the effect of runway or deck surface, sinking speed, and tire pressure on the spin-up coefficients of friction. Also presented are some data on the landing-gear response to impacting on and taxiing over a $1\frac{3}{8}$-inch-diameter arresting gear cable stretched across the nonskid carrier deck surface.

SYMBOLS

F_H	horizontal (drag) force, lb
F_V	vertical force, lb
I	moment of inertia, slug-ft^2
p_o	tire-inflation pressure (unloaded), lb/sq in.
r_o	unloaded tire radius, ft
S	length of strut stroke, ft
T	temperature of runway surface, ^oF
t	time after touchdown, sec

V_H	horizontal velocity at touchdown, knots
V_V	vertical velocity at touchdown, ft/sec
w	weight, lb
$\ddot{x}$	horizontal acceleration, gravity units
$\ddot{z}$	vertical acceleration, gravity units
δ	tire deflection, ft
θ	wheel angular displacement, revolutions
μ	instantaneous tire-surface friction coefficient, $F_{H,g}/F_{V,g}$
φ	angle between shock-strut axis and vertical, deg
ω	wheel angular velocity, radians/sec

Subscripts:

a	axle
avg	average (over spin-up time history)
g	ground
m	determined at time of maximum horizontal ground load
o	initial value at touchdown
t	time after touchdown
1	upper mass
2	lower mass
3	wheel and axle mass

APPARATUS

Test Vehicle

The tests were carried out by making simulated landings and taxiing runs at the Langley landing loads track. The arrangement of the basic elements of this facility is shown schematically in figure 1. The large main carriage weighs approximately 100,000 pounds (fig. 2) and rides on 6-inch-square continuous steel rails located on each side of a 2,200-foot-long concrete runway. Located within this main carriage and traveling on vertical rails is the drop carriage to which the landing gear (fig. 3) is attached.

Simulated landings were made by accelerating the main carriage to the desired forward speed by means of the hydraulic jet catapult (ref. 5) and then releasing the drop carriage which was initially set at a height based on the vertical velocity desired for the test. A constant lift force approximately equal to the dropping mass (1 g wing lift) was applied to the drop carriage when the desired vertical velocity was reached. This force was applied throughout the impact. The taxiing tests were made with zero wing lift.

Runway Surface

Figure 4 shows the nonskid carrier deck installed on the track runway. This deck was fabricated from 1/4 inch thick by 18 inches wide steel boiler plate sections that were welded end to end to form a continuous strip approximately 200 feet long. Relative motion between the deck and runway surfaces during an impact was prevented by the steel clips attached to the edges of the nonskid deck shown in figure 4.

Two coats of a nonskid compound were troweled upon the top of this decking according to instructions given for the application of this compound to carrier decks. This compound conformed to the specifications given in reference 6 for a nonslip, lightweight, and abrasive-filled synthetic binder-type flight deck compound.

Local asperities in the concrete runway prevented the test nonskid deck from lying absolutely flush with the concrete surface. As can be seen from figure 5, the magnitude of these asperities was at least as large as 0.09 inch. Because of this condition, some small local deformations to the steel deck probably occurred during an impact. It should be pointed out that an actual carrier deck during an impact would probably encounter much larger local deflections due to its less stiff construction. No attempt was made, in this investigation, however, to assess the effect of deck deflection on the test results.

The runway was made from Portland cement concrete and its surface texture is similar to Portland Cement Concrete runways in general use today. For comparison purposes, a typical profile of the impact area concrete runway surface (obtained from a plaster impression) is shown in figure 5 along with a cross section of the nonskid carrier deck. This figure shows that the nonskid deck was much more regular than the concrete surface.

At the conclusion of the simulated landings on the concrete and nonskid deck surfaces, several additional tests were made where the test landing gear impacted on and taxied across a $1\frac{3}{8}$-inch-diameter steel arresting cable that was stretched across and rigidly attached (welded) to the nonskid carrier deck. This installation is shown in figure 6.

Landing Gear

The test landing gear (fig. 3) was a standard production gear that is in use as the main landing gear on a carrier jet attack airplane which has a gross weight ranging between 16,000 and 20,000 pounds. The weight of the total dropping mass including landing gear used in this investigation was approximately 6,630 pounds.

The landing gear was set at an inclination of 2.5° from the vertical (normal airplane landing attitude) for the simulated landings on concrete. Gear inclinations of 2.5° forward and 5.1° rearward (3-point attitude) were used for simulated landings on the carrier deck. The landing gear was carefully positioned beneath the drop carriage such that the yaw angle and roll angles were zero. However, the unsymmetrical location of the wheel axle with respect to the strut axis and the structural flexibility of the landing gear were such that the rolling and yawing moments produced by the tire forces on the gear introduced substantial wheel tilting and yawing motions during impact.

The spot brake assembly including the brake disk was removed from the gear in order to install the lower mass accelerometers. Weight was added to the axle brake flange (in form of a steel plate) and to the wheel (steel ring) in order to approximate the gear lower and rotational masses with brake assembly installed. The lower mass (lower shock strut, wheel, and tire) weighed approximately 126 pounds. A shock-strut inflation pressure (strut extended) of 55 pounds per square inch was used throughout the investigation.

Tire

The tire (fig. 3) used in this investigation was a 24 × 5.5, type VII, 14 ply-rating rib-tread tire. According to reference 7, the rated static load for this tire is 9,700 pounds at a tire-inflation pressure of 300 pounds per square inch. The weight of the rotating mass (wheel, tire, instrumentation, and axle) was 78 pounds. The moment of inertia of the rotating mass was 0.784 slug-ft^2. Tire pressures of 260, 320, and 400 pounds per square inch were investigated.

Instrumentation

The base of the lower shock strut in the vicinity of the axle juncture with the strut (see fig. 3(b)) was mounted with strain gages by the airplane manfacturer to measure forces parallel and normal to the strut axis. The position of the strain gages on the strut was selected according to procedures outlined in reference 8. These procedures determined strain-gage locations on the strut such that the gage responses to loads other than the primary load were at a minimum.

The applied ground forces were determined by correcting the axle strain-gage loads for the effects of inertia forces introduced by the wheel and other masses attached to the axle outboard of the strain gages (force at ground equal to sum of axle strain-gage force and product of total mass outboard of axle strain gages and the acceleration of this mass). These corrections were obtained from accelerometers installed on the brake flange plate and inside the hollow axle at the tire center line. These accelerometers were oriented so that they measured vertical and horizontal accelerations, respectively, for the 2.5° forward landing-gear inclination.

The drop carriage is equipped with a six-component dynamometer (fig. 3(c)) to measure loads and moments imparted by the landing gear. Corrections to the dynamometer loads for the inertia forces introduced by the upper (attachment fixture and outer shock strut) and lower (inner shock strut, wheel, and tire) masses attached to the dynamometer were derived from acceleration values of the upper and lower mass accelerometers, respectively. The two upper mass accelerometers mounted between the stiffeners of the landing-gear attachment plate of the attachment fixture (fig. 3(d)) were oriented to measure vertical and horizontal (drag) accelerations. The two lower mass accelerometers are shown in figure 3(d) and were mounted on the brake flange plate. These accelerometers were oriented 90° apart to measure vertical and horizontal accelerations for the 2.5° forward landing-gear inclination. It should be noted that the lower mass vertical accelerometer just discussed is the same instrument that was used to obtain the vertical inertia-force correction for the vertical strain-gage load.

The ground drag load was also determined from values of acceleration measured by the angular accelerometer, mounted under the landing-gear wheel cover on the wheel (fig. 3(a)), according to the method discussed in references 4 and 9. The wheel was also instrumented to measure angular velocity and displacement.

TEST PROCEDURE

Before each simulated landing run, the landing surface was cleaned and its condition of wetness or dryness noted. The surface temperature of the landing area was measured by means of a mercury thermometer (shaded from the sun). The landing-gear wheel was enclosed in a canvas bag that was secured by a rope to a fixed portion of the main carriage structure in order to protect the tire from the water spray emanating from the jet catapult during the accelerating portion of the run. This bag was retracted from the tire (just before touchdown) during the coasting portion of the run (jet catapult cut off) while the landing gear was being accelerated vertically by the action of gravity in order to acquire the desired vertical velocity at touchdown. Immediately after a run the touchdown area of the runway was examined and the condition of wetness noted.

For some runs, this bag did not fully protect the tire from the water spray (tire became wet) and the initial tire contact region on the dry runway would be either wet or damp. It should also be noted that, for a few runs, the operating conditions of the jet catapult and the velocity and direction of the wind at the time of a run combined to produce a condition in which the water spray from the jet overran the main carriage and contaminated (wetted) the runway impact region ahead of touchdown.

The canvas bag was not used to protect the tire from water spray during the taxiing over cable runs. With this exception, the taxiing runs were conducted in a manner similar to the simulated landing runs.

The results of studies made of high-speed motion-picture film taken of each run along with the observations on runway and tire wetness made before and after a run determined the approximate wetness values for the tire and runway listed in tables I to III for each run.

Simulated Landings on Concrete and on Nonskid Deck Surfaces

A series of 15 landings was made to establish the friction-coefficient characteristics developed between the tire and concrete runway. These tests were made with the shock strut inclined 2.5° forward of the vertical for vertical velocities at touchdown of approximately 12 and 16 feet per second and for initial tire-inflation pressures of

260, 320, and 400 pounds per square inch. The forward or horizontal speed at touchdown ranged between 76 and 93 knots for these runs.

A series of 24 landings was made to establish the friction-coefficient characteristics developed between the tire and the nonskid carrier deck. Most (15) of these landings were made with the shock strut inclined 2.5° forward of the vertical for tire-inflation pressures of 260, 320, and 400 pounds per square inch and for vertical velocities at touchdown ranging from approximately 12 to 19 feet per second. The horizontal velocity at touchdown ranged between 83 and 104 knots for these landings. The remaining 9 landings on the nonskid deck were made with the shock strut inclined 5.1° rearward of the vertical for a tire-inflation pressure of 320 pounds per square inch. Vertical and horizontal velocities for these landings ranged between approximately 12 and 19 feet per second and 54 and 102 knots, respectively.

L
4
6
0

Landing and Taxiing Over $1\frac{3}{8}$-Inch-Diameter Steel Arresting Cable

A series of 3 landings was made on the arresting cable stretched across the nonskid carrier deck (fig. 6) under conditions of $\varphi = 2.5°$ forward, $V_V \approx 12$ feet per second, $V_H \approx 98$ knots, and $p_o = 400$ pounds per square inch. These landings were arranged such that touchdown on the cable occurred before maximum ground horizontal load, during maximum horizontal ground load, and during maximum vertical ground load on the landing gear.

In addition to these runs, 4 taxiing runs (Wing lift = 0, $V_V = 0$) were also conducted over the arresting cable. Test conditions for these runs were $p_o = 260$, 320, and 400 pounds per square inch.

RESULTS AND DISCUSSION

The test landing gear was mounted with strain gages by the airplane manufacturer primarily for use in future flight tests to be conducted after the conclusion of the present investigation. Since the accuracy of strain-gage-type ground-load measurements during flight tests in the past have been relatively poor, the accuracy of the test axle strain-gage installation was evaluated by comparing the strain-gage results with the results from the standard track instrumentation.

Figure 7 presents a comparison of loads and friction coefficients determined from the carriage dynamometer, axle strain gages, and wheel angular accelerometer along with appropriate inertia corrections for a sample simulated landing. This figure shows that good agreement exists between the different ground-loads measurements throughout most of the impact time history. The reliability of the horizontal ground-load measurement (axle-strain-gage method) was also confirmed by data obtained from other test instrumentation as is shown in figure 8. Figure 8 compares the change in momentum of the wheel with the ground drag torque impulse acting on the wheel for a typical impact time history. The data shown in this figure were obtained by use of the relationship

$$\int_0^t F_{H,g}\left(r_o - \delta\right)dt = I\left(\omega_t - \omega_o\right)$$

Analysis of the data shown in figures 7 and 8 along with other similar data indicated that the best representation of the applied ground forces developed on the test landing gear during an impact was actually obtained from the axle strain-gage measurements rather than from the standard track instrumentation (carriage dynamometer). This conclusion was based on the fact that the carriage-dynamometer measurements had to undergo two separate inertia-force corrections (upper and lower mass) to arrive at the applied ground forces. The axle strain gages, on the other hand, had to be corrected only for the acceleration of the smaller wheel and tire mass located outboard of these strain gages. Consequently, the axle strain-gage measurements would be affected the least by any errors developed in deriving these inertia-force corrections.

The test results indicate that, for the test landing gear, the method of reference 8 produced strain-gage locations that were free from large load interactions and that, when corrected for effects of inertia forces, accurately represented the applied ground forces developed on impact up through wheel spin-up.

Except for the data in figures 7 and 8, all ground forces and friction-coefficient data in this paper were derived from the axle strain-gage method since, as just explained, it is believed that this method generally produced the most accurate representation of the ground forces acting on the tire.

It should be noted that, for some simulated landing impacts, the maximum coefficient of friction did not occur at the time of maximum ground drag load. The maximum coefficient-of-friction values for these particular runs generally occurred at a time when the inertia-force corrections to the axle strain-gage loads were either relatively large or changing rapidly. Because of these large corrections, a slight

difference in phasing between the accelerometer and strain-gage responses would affect the derived friction coefficient considerably. In order to minimize the effects of these corrections, the correlation of the data in this paper is based on the friction coefficients developed at time after touchdown of maximum ground drag load rather than the maximum values. At this particular time during the impact (see fig. 7) the inertia-force corrections to the strain-gage loads are of small or negligible magnitude and phase differences in the instrumentation would have little or no effect on the friction coefficient.

Tables I and II summarize all test data obtained from the simulated landings on the concrete and nonskid deck surfaces that were determined at the instant of maximum ground drag load. Also given in these tables are the values of the average spin-up friction coefficient μ_{avg} developed during these landings. L 4 6 0

Effects of Surface and Surface Wetness

Figure 9 compares ground-load and friction-coefficient time histories developed during landings on the concrete and nonskid deck surfaces at a sinking speed of approximately 12 feet per second and tire-inflation pressures of 260, 320, and 400 pounds per square inch. Similar time histories are presented in figure 10 for landings on the concrete and nonskid deck surfaces made at a sinking speed of approximately 16 feet per second.

An attempt was made to conduct this investigation on dry tire and runway surfaces. As previously explained in the test procedure, the precautions taken before and during a run to permit testing on a dry surface were not always successful and for some runs either or both the tire and runway surfaces were contaminated to some degree with water at time of touchdown. It was impossible to denote quantitatively the amount of water present during these runs; however, a qualitative wetness value is listed for each run in tables I to III by the use of terms such as wet, damp, dry, and so forth.

The data given in tables I and II and figures 9 and 10 indicate that the presence of water on either or both the tire and the different runway surfaces generally resulted in decreasing both the average friction coefficient μ_{avg} and the friction coefficient at time of maximum ground drag load μ_m and increasing the time required for wheel spin-up. These data also tend to indicate that these effects become more pronounced as the amount of water between the tire and runway surface is increased.

The comparison of matched landings on the concrete and nonskid deck surfaces presented in figures 9 and 10 indicates that the instantaneous

tire-surface friction coefficients μ developed on the nonskid deck are considerably lower than those developed on the concrete runway under similar landing conditions. The data shown in these figures and in tables I and II also indicate that the time required to reach wheel spin-up is consiberably longer for landings on the nonskid deck than for landings of similar horizontal velocity on the concrete runway. Since the change in momentum required of the wheel is the same for landings of equal horizontal velocity, a longer time to wheel spin-up requires the torque impulse $\int_0^t \mu F_{V,g}(r_o - \delta)dt$ acting on the wheel to be conducted at lower level or with a lower friction coefficient μ.

As would be expected from this discussion, the experimental data also indicated that values of tire-surface friction coefficient at time of maximum ground drag load μ_m and the average tire-surface friction coefficient μ_{avg} developed on the nonskid deck are considerably lower than the matching values developed on the concrete runway. The lower friction coefficients obtained on the nonskid deck are believed to be in part due to the much more regular surface of the nonskid deck as compared with the 0.09-inch deviations of the concrete runway. (See fig. 5.)

Effect of Strut Inclination

Figure 11 compares ground-load and friction-coefficient time histories of landings on the nonskid deck made at the two strut inclinations tested. Care was taken in this figure to match runs having approximately equal conditions of V_V, V_H, and p_o so that the effect of strut inclination on the ground loads and friction coefficient during landing on the nonskid carrier deck could be evaluated.

It can be seen from the data shown in figure 11 that the landings on the nonskid deck made at the airplane 3-point attitude ($\varphi = 5.1^\circ$ rearward) experienced considerably more strut binding or friction during the impact than did the landings made at the normal airplane landing attitude ($\varphi = 2.5^\circ$ forward). This observation was suggested by the larger vertical and horizontal ground loads occurring to the 3-point landings during wheel spin-up. These data also indicate that the effect of strut inclination on the tire-surface friction coefficients was small or negligible for the conditions tested.

Effect of Forward Speed

Ground-load and friction-coefficient time histories obtained from landings made on the nonskid deck at forward speeds ranging from 54.4 to 98.9 knots and having approximately identical conditions of V_V, p_o, and φ are shown in figure 12. The variation of both μ_m and μ_{avg} with forward speed is shown in figure 13 for all landings (10) on the concrete and nonskid deck surfaces made at sinking speed of approximately 16 feet per second.

The data shown in figures 12 and 13 indicate that the spin-up friction coefficients μ, μ_m, and μ_{avg} developed between the tire and both test surfaces tended to decrease in magnitude with increasing forward speed. This result is in agreement with results reported earlier in references 1 and 4 for landings on concrete surfaces.

L
4
6
0

Effect of Vertical Velocity

The effect of vertical velocity on the ground loads and friction coefficients developed during landings made on the concrete and nonskid deck surfaces illustrated by the data shown in figures 14 and 15. These data indicate the μ, μ_m, and μ_{avg} decreased with increasing vertical velocity for the simulated landings on the nonskid deck over the range of vertical velocitites tested (12 to 19 feet per second). This trend was not so clearly defined for the landings on the concrete runway because of the limited data (only two vertical velocities tested, 12 and 16 feet per second) and effects of water contamination of the scrubbing surfaces.

Effect of Tire Pressure

The variation of spin-up friction coefficients developed between the tire and the test runway surfaces with tire-inflation pressure is somewhat obscured by the effects of surface wetness on the test results. A trend for μ_m to decrease very slightly with increasing tire inflation pressure for the concrete and nonskid deck surfaces is apparently indicated in figure 16. However, the experimental data seem to indicate, in general, that the spin-up friction coefficients, that is, μ, μ_m, and μ_{avg}, are relatively independent of tire-inflation pressure for the tire-inflation pressure range (260 to 400 pounds per square inch) tested.

Landing and Taxiing Over $1\frac{3}{8}$ - Inch-Diameter Steel Arresting Cable

Three landings were made on the arresting cable stretched across the nonskid carrier deck (fig. 6) under conditions of $\varphi = 2.5^{\circ}$ forward, $V_V \approx 12$ feet per second, $V_H \approx 98$ knots, and $p_o = 400$ pounds per square inch. These three landings were arranged such that cable runover occurred (1) before maximum ground horizontal load, (2) during maximum horizontal ground load, and (3) during maximum vertical ground load on the landing gear. Time histories of the loads and accelerations experienced by the gear during these landings are compared with an equivalent landing on the nonskid deck time history (run 22) in figures 17 to 19. The incremental load increases experienced by the gear during cable run over, obtained from figures 17, 18, and 19, are listed in table III.

Four runs were also made during which the landing gear was taxied across this cable under conditions of zero vertical velocity and zero wing lift. Table III lists the incremental load increases over static load $\left(F_{V,static} = 6{,}630 \text{ lb}\right)$ developed while crossing the cable for these runs. Time histories of loads and accelerations experienced by the gear while taxiing over the cable are given in figures 20 and 21.

The data given in figures 17 to 21 along with table III indicate that the maximum incremental vertical and horizontal loads developed at either the landing gear or at the ground by impacting on or taxiing over the arresting cable did not exceed about two-thirds of the static load $\left(F_{V,static} = 6{,}630 \text{ lb}\right)$ on the landing gear axle for the conditions tested.

It should be mentioned, however, that these incremental loads would not be representative of landings and taxiing runs having conditions under which the tire would be bottomed or at a near bottomed condition at time of cable runover. Much larger incremental loads would be experienced by the landing gear under such conditions since the tire would no longer have the required deflection potential remaining to absorb or swallow the cable.

CONCLUSIONS

Simulated landings using a landing gear of 6,630-pound static-load rating were made on concrete and nonskid deck surfaces over test ranges from 54 to 104 knots horizontal velocity and from 12 to 19 feet per second vertical velocity at touchdown for tire-inflation pressures

of 260, 320, and 400 pounds per square inch. In addition, several simulated landing (zero vertical velocity) tests were conducted on a $1\frac{3}{8}$-inch-diameter steel arresting cable for approximately the same range of horizontal velocity. The results of these tests indicated the following conclusions:

1. The spin-up friction coefficients, μ, μ_{avg}, and μ_m, developed on the nonskid deck were found to be considerably less than those developed for similar landings on concrete for the conditions tested.

2. The presence of water on either or both the tire and the test surfaces at touchdown tended to decrease the magnitude of the spin-up friction coefficients and to increase the time required for wheel spin-up over the range of conditions tested.

3. The spin-up friction coefficients developed on the test surfaces tended to decrease with both increasing horizontal and vertical velocity at touchdown over the test range.

4. The spin-up friction coefficients developed on the test surfaces appeared to be relatively independent of both tire inflation pressure and strut inclination for the conditions tested.

5. The maximum incremental vertical and horizontal loads generated by crossing the cable during simulated landing and taxiing tests did not exceed about two-thirds of the static load (6,630 pounds) on the landing gear.

Langley Research Center,
National Aeronautics and Space Administration,
Langley Field, Va., October 27, 1959.

REFERENCES

1. Milwitzky, Benjamin, Lindquist, Dean C., and Potter, Dexter M.: An Experimental Study of Applied Ground Loads in Landing. NACA Rep. 1248, 1955. (Supersedes NACA TN 3246.)

2. Hall, Albert W., Sawyer, Richard H., and McKay, James M.: Study of Ground-Reaction Forces Measured During Landing Impacts of a Large Airplane. NACA TN 4247, 1958. (Supersedes NACA RM L55E12C.)

3. Batterson, Sidney A.: Recent Data on Tire Friction During Landing. NACA RM L57D19b, 1957.

4. Batterson, Sidney A.: Investigation of the Maximum Spin-up Coefficients of Friction Obtained During Tests of a Landing Gear Having a Static-Load Rating of 20,000 Pounds. NASA MEMO 12-20-58L, 1958.

5. Joyner, Upshur T., and Horne, Walter B.: Considerations on a Large Hydraulic Jet Catapult. NACA TN 3203, 1954. (Supersedes NACA RM L51B27.)

6. Anon.: Report of Evaluation XPA 422047 Flight Deck Compound Lab. Proj. 5426, Prog. Rep. 13, Material Lab., New York Naval Shipyard Feb. 10, 1956.

7. Anon.: Casings, Tire and Tubeless Tires; Aircraft Pneumatic. Military Specification, MIL-C-5041B, Feb. 5, 1957.

8. Meriwether, Harry D.: A Method of Instrumenting and Calibrating Main Gears for Carrier Suitability Trials. Paper presented to the Society for Experimental Stress Analysis (San Diego, California), Mar. 8, 1957.

9. Theisen, Jerome G., and Edge, Phillip M., Jr.: An Evaluation of an Accelerometer Method for Obtaining Landing-Gear Drag Loads. NACA TN 3247, 1954.

TABLE I.- CONCRETE-RUNWAY DATA

[φ = 2.5° forward; 1 g wing lift]

Initial conditions at touchdown							Values measured at time of maximum ground drag load							μ_{avg}
Run	p_o, lb/sq in.	V_V, ft/sec	V_H, knots	Tire	Runway		t_m, sec	$F_{V,g,m}$, lb	$F_{H,g,m}$, lb	μ_m	S_m, ft	δ_m, ft	θ_m, rev	
					Condition	T, °F								
1	260	11.9	91.1	Wet	Dry	43	0.0350	10,800	6,150	0.57	0.29	0.10	0.29	0.42
2	260	12.5	94.8	Damp or dry	Dry	56	.0300	10,000	6,100	.61	.23	.11	.19	.43
3	260	12.6	79.6	Dry	Dry	57	.0275	9,100	5,900	.65	.22	.10	.16	.42
4	260	15.9	76.7	Dry	Dry	60	.0200	8,850	7,550	.85	.18	.12	.10	.43
5	260	16.1	96.3	Dry	Dry	64	.0250	12,400	8,050	.65	.22	.16	.20	.39
6	320	12.3	79.6	Dry	Dry	52	.0250	8,150	5,700	.70	.21	.08	.17	.47
7	320	12.5	90.4	Damp or dry	Dry	54	.0325	10,200	5,850	.57	.28	.09	.25	.39
8	320	12.5	79.2	Wet	Wet	(a)	.0330	10,300	5,000	.47	.29	.07	.26	.32
9	320	15.9	76.5	Wet	Dry	60	.0220	13,600	7,600	.56	.17	.17	.16	.48
10	320	16.1	92.4	Damp or dry	Damp or dry	54	.0275	13,300	7,950	.60	.31	.08	.20	.38
11	320	16.4	76.0	Dry	Dry	50	.0200	10,300	8,150	.79	.18	.11	.11	.42
12	400	12.0	92.7	Damp or wet	Damp or wet	50	.0375	11,250	5,800	.52	.31	.05	.30	.37
13	400	12.3	83.6	Wet	Dry	58	.0250	9,350	5,400	.58	.23	.06	.14	.41
14	400	15.8	84.2	Wet	Dry	52	.0250	14,050	7,750	.55	.24	.10	.18	.35
15	400	16.0	96.6	Wet	Dry	59	.0225	14,750	9,000	.61	.23	.11	.19	.39

[a] Not measured.

TABLE II.- NONSKID CARRIER DECK DATA FOR 1 g WING LIFT

(a) $\varphi = 2.5^{\circ}$ forward

Initial conditions at touchdown							Values measured at time of maximum ground drag load							μ_{avg}
Run	P_o, lb/sq in.	V_V, ft/sec	V_H, knots	Tire	Runway condition	Runway T, °F	t_m, sec	$F_{V,g,m}$, lb	$F_{H,g,m}$, lb	μ_m	S_m, ft	δ_m, ft	θ_m, rev	
16	260	12.5	100.4	Dry	Dry	59	0.0475	11,100	5,900	0.53	0.40	0.11	0.39	0.31
17	260	15.9	95.3	Dry	Dry	73	.0350	14,850	6,450	.43	.35	.13	.30	.28
18	320	12.4	92.6	Wet	Dry	61	.0675	11,200	4,450	.40	.63	.12	.51	.20
19	320	16.0	95.3	Wet	Dry	63	.0350	14,800	6,800	.46	.36	.16	.27	.30
20	320	17.0	97.2	Wet	Dry	54	.0425	17,950	5,650	.32	.45	.22	.38	.26
21	320	17.3	103.4	Damp or dry	Dry	54	.0350	18,800	7,200	.38	.37	.17	.34	.29
22	400	12.3	97.0	Dry	Dry	73	.0425	11,400	5,600	.49	.37	.13	.32	.30
23	400	12.6	90.7	Damp or wet	Dry	75	.0500	12,100	4,400	.37	.48	.12	.35	.23
24	400	16.3	92.7	Damp or wet	Dry	74	.0375	18,150	6,350	.35	.40	.15	.33	.27
25	400	16.5	83.3	Damp or dry	Dry	77	.0350	16,600	6,000	.36	.37	.14	.24	.25
26	400	17.1	99.1	Damp	Damp	53	.0400	19,050	7,050	.37	.44	.19	.32	.22
27	400	17.3	104.3	Dry	Dry	55	.0425	19,600	7,050	.36	.48	.21	.42	.22
28	400	17.3	103.2	Dry	Dry	54	.0375	19,100	7,650	.40	.40	.17	.34	.28
29	400	18.5	86.6	Wet	Dry	70	.0450	20,450	6,200	.30	.58	.20	.31	.15
30	400	19.1	95.6	Wet	Damp or dry	85	.0425	23,200	5,950	.26	.52	.23	.37	.20

(b) $\varphi = 5.1^{\circ}$ rearward

Initial conditions at touchdown							Values measured at time of maximum ground drag load							μ_{avg}
Run	P_o, lb/sq in.	V_V, ft/sec	V_H, knots	Tire	Runway condition	Runway T, °F	t_m, sec	$F_{V,g,m}$, lb	$F_{H,g,m}$, lb	μ_m,	S_m, ft	δ_m, ft	θ_m, rev	
31	320	12.5	91.2	Damp or wet	Dry	85	0.0600	13,250	5,500	0.42	0.54	0.16	0.46	0.22
32	320	15.6	69.5	Dry	Dry	91	.0250	12,900	6,700	.52	.21	.16	.14	.29
33	320	15.9	75.4	Damp or dry	Dry	95	.0300	17,550	6,000	.34	.27	.20	.20	.25
34	320	16.3	98.9	Wet	Dry	93	.0425	21,200	6,350	.30	.43	.21	.35	.25
35	320	16.4	95.3	Dry	Dry	85	.0425	18,700	7,500	.40	.39	.22	.35	.27
36	320	16.4	54.4	Dry	Dry	80	.0175	11,250	6,650	.59	.13	.12	.06	.28
37	320	17.0	93.5	Damp or dry	Dry	79	.0350	20,000	7,200	.36	.33	.19	.29	.27
38	320	18.1	102.1	Dry	Dry	92	.0375	23,350	8,900	.38	.36	.27	.32	.25
39	320	19.0	91.7	Damp	Damp	93	.0350	22,700	7,500	.33	.36	.24	.28	.23

TABLE III.- LOADS GENERATED BY CROSSING $1\frac{3}{8}$-INCH-DIAMETER ARRESTING CABLE

(a) Impact tests: $\varphi = 2.5^{\circ}$ forward; $p_o = 400$ lb/sq in.;
Wing lift = 1 g; nonskid carrier deck

Initial conditions at touchdown						Crossing of cable occurred -	Maximum incremental load increase crossing cable			
Run	V_V, ft/sec	V_H, knots	Tire	Runway	T, $^{\circ}F$		$F_{V,a}$	$F_{V,g}$	$F_{H,a}$	$F_{H,g}$
40	12.5	99.0	Dry	Dry	89	Before $F_{H,g,max}$	2,800	4,000	3,600	4,200
41	12.3	93.8	Dry	Dry	(a)	At $F_{H,g,max}$	2,500	3,000	6,200	5,900
42	12.2	100.7	Dry	Dry	(a)	At $F_{V,g,max}$	3,800	4,900	2,400	2,000

[a]Not measured.

(b) Taxiing tests: $V_V = 0$; $F_{V,static} = 6,630$ lb;
Wing lift = 0; nonskid carrier deck

Initial conditions							Maximum incremental load increase crossing cable			
Run	p_o, lb/sq in.	V_H, knots	φ, deg	Tire condition	Runway condition	T, $^{\circ}F$	$F_{V,a}$	$F_{V,g}$	$F_{H,a}$	$F_{H,g}$
43	400	97.7	2.5 forward	Dry	Dry	(a)	3,500	4,600	1,150	1,600
44	400	89.9	5.1 rearward	Dry	Dry	76	2,700	3,700	1,650	1,600
45	320	86.8	5.1 rearward	Wet	Wet	(a)	2,100	2,600	1,250	1,350
46	260	83.2	5.1 rearward	Wet	Wet	(a)	1,500	1,900	1,250	1,700

[a]Not measured.

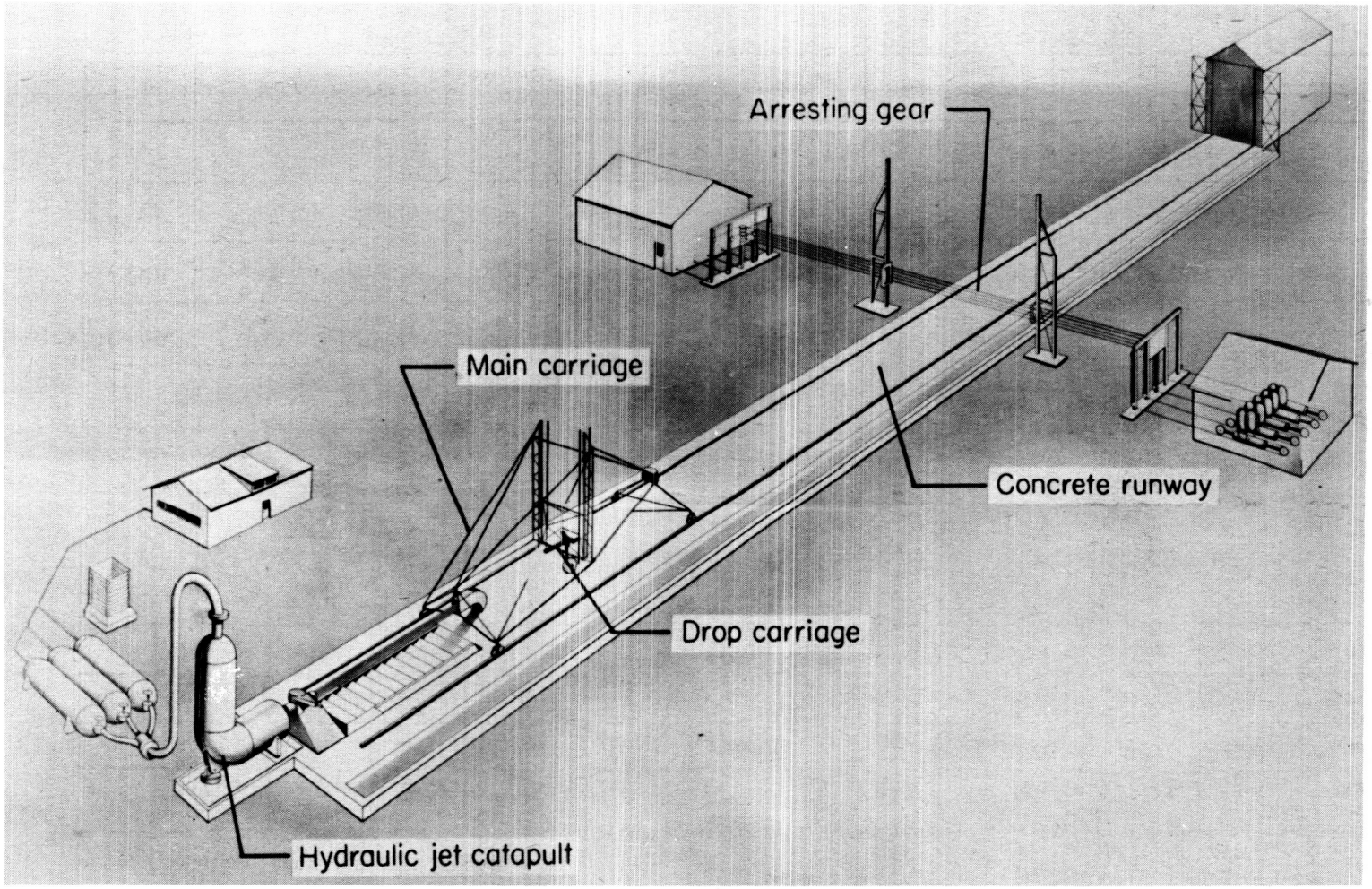

Figure 1.- Schematic drawing of Langley landing loads track. L-58-1693

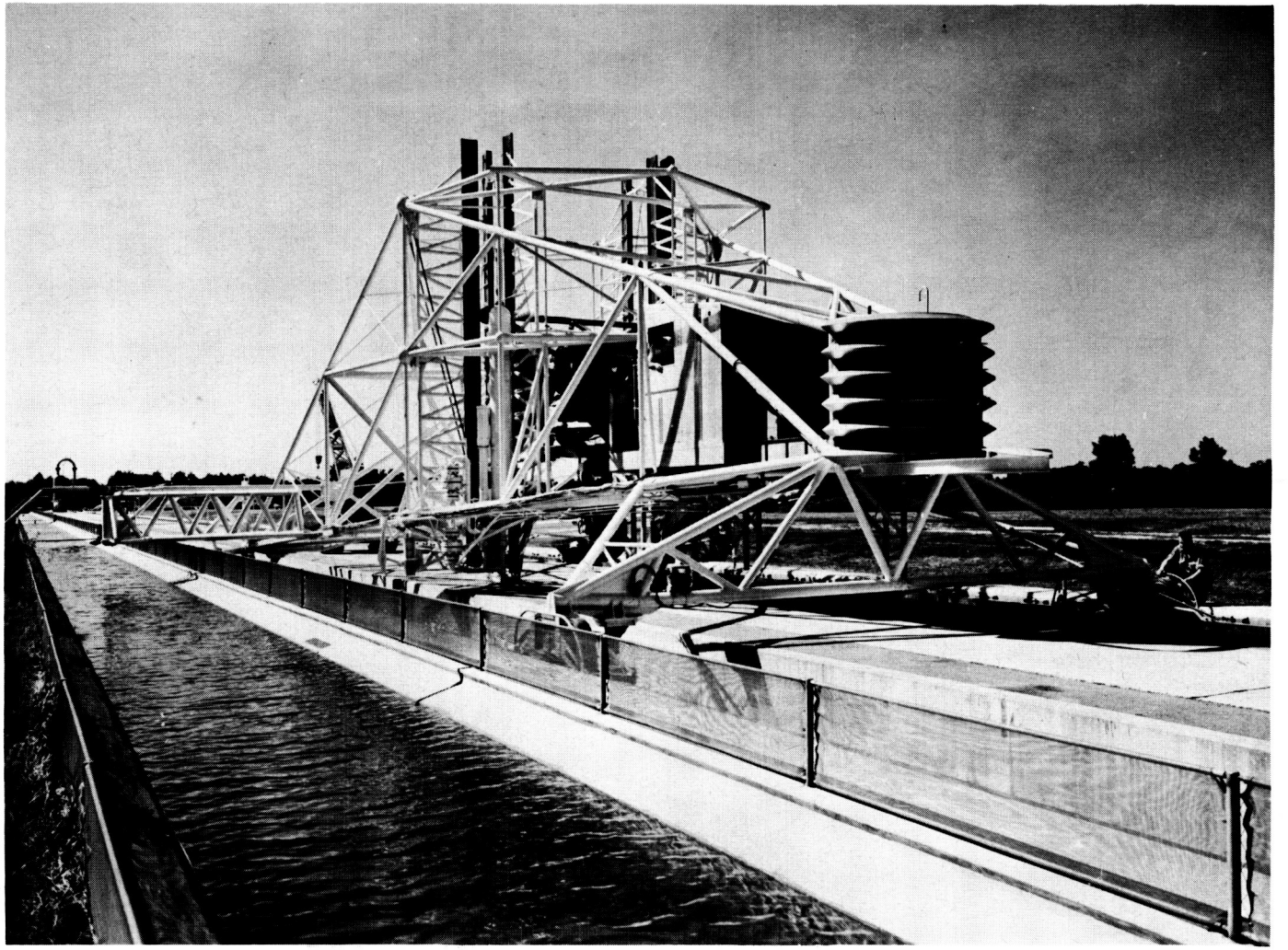

Figure 2.- Landing loads track carriage. L-95476

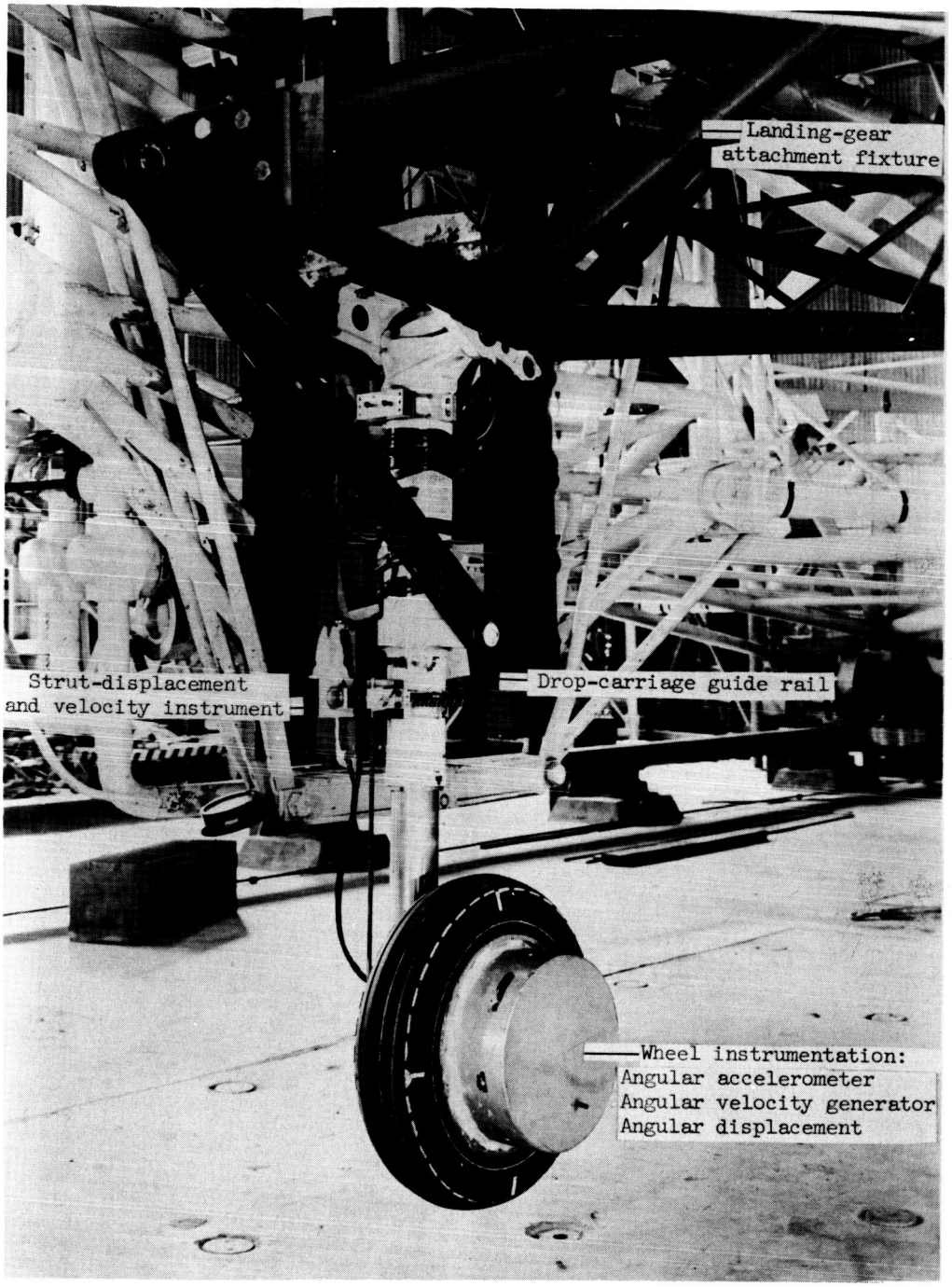

(a) Strut inclination $2^{\circ}30'$ forward; side view. L-58-1135.1

Figure 3.- Landing gear mounted for testing.

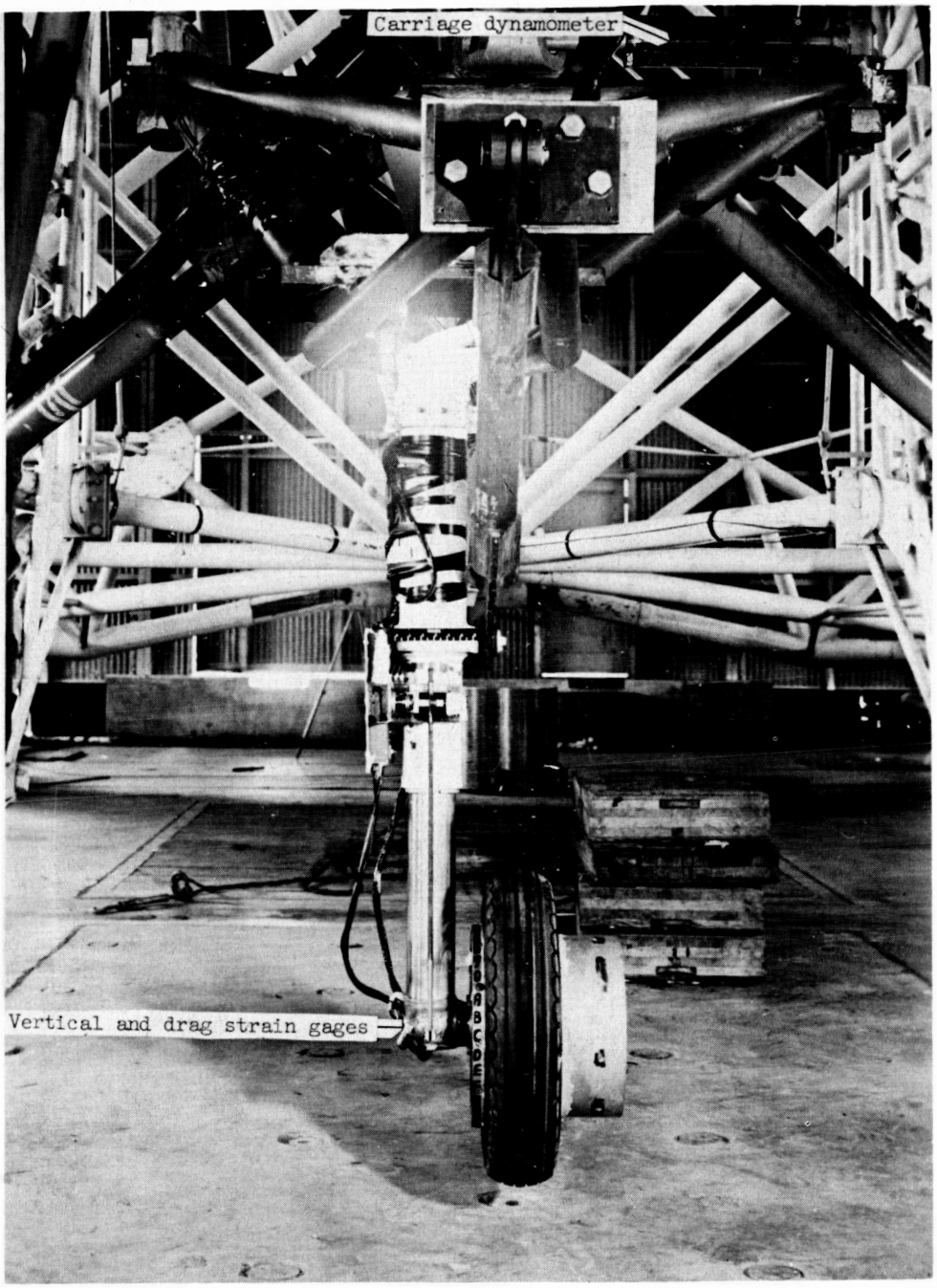

(b) Strut inclination 2°30' forward; front view. L-58-1136.1

Figure 3.- Continued.

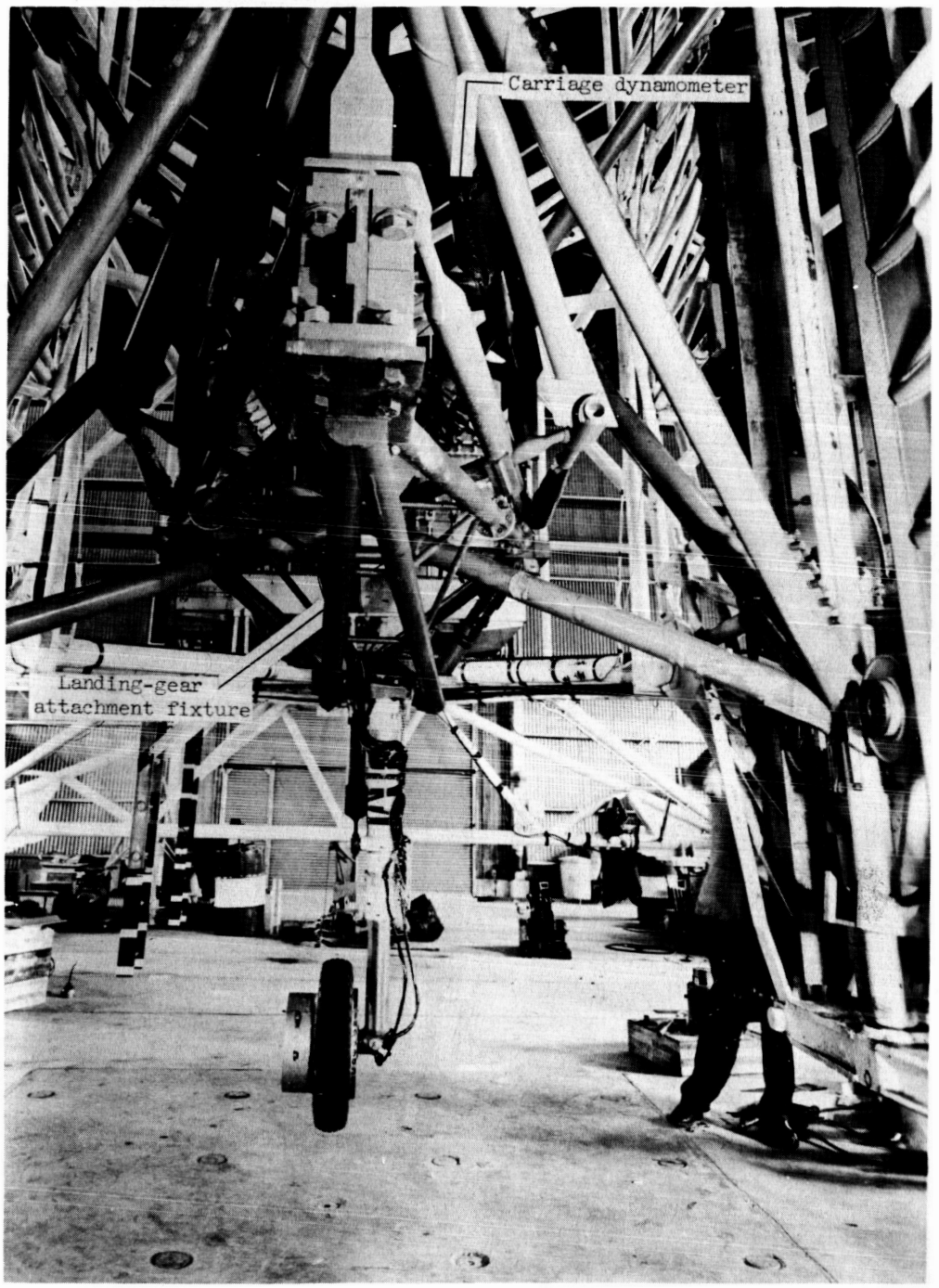

(c) Strut inclination $2^{\circ}30'$ forward; rear view. L-58-1134.1

Figure 3.- Continued.

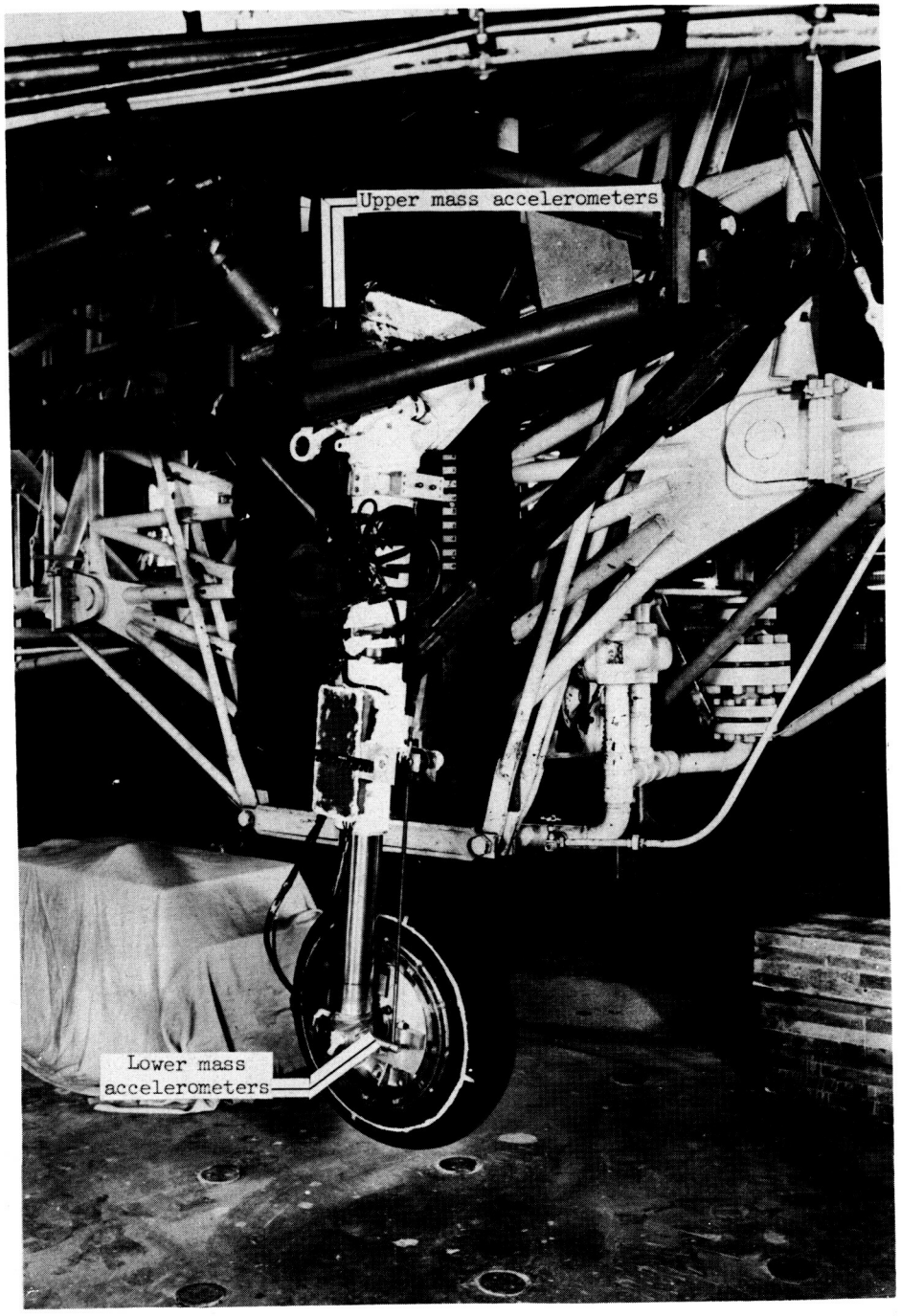

(d) Strut inclination $5^{\circ}5'$ rearward; side view. L-58-1758.1

Figure 3.- Concluded.

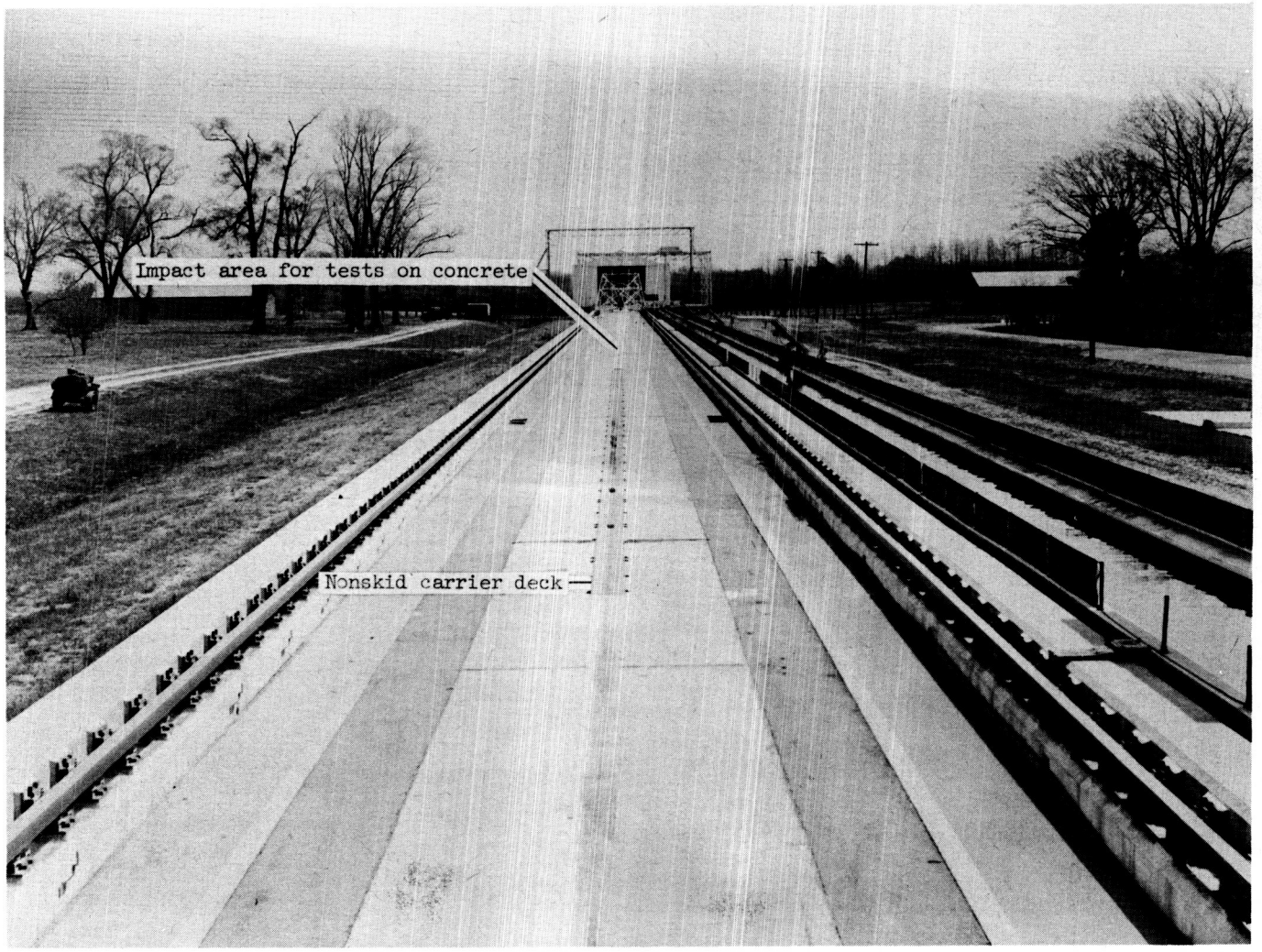

Figure 4.- Nonskid carrier deck installation on Langley landing loads track. L-58-1599.1

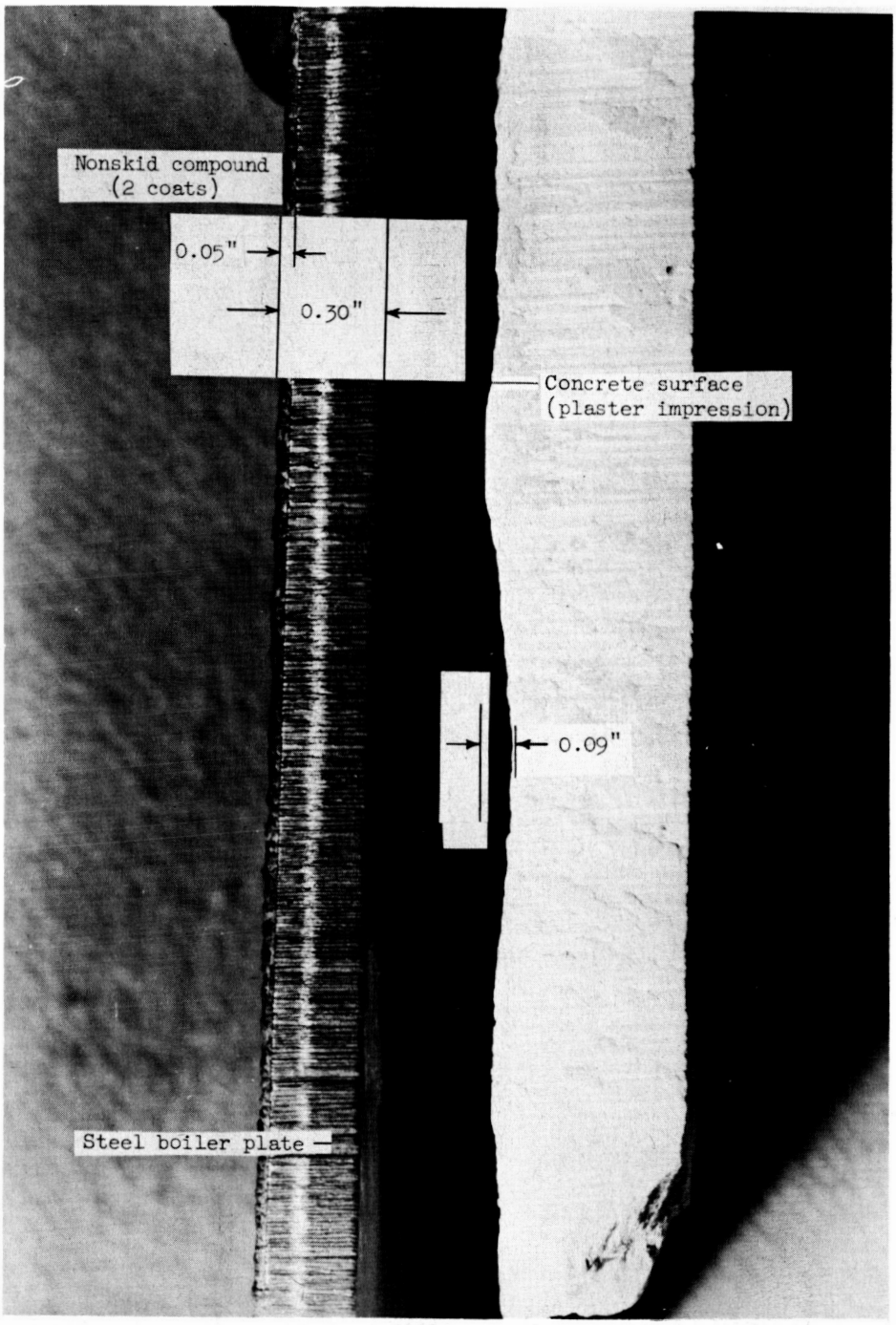

L-59-653.1

Figure 5.- Comparison of nonskid carrier-deck and concrete-runway surfaces.

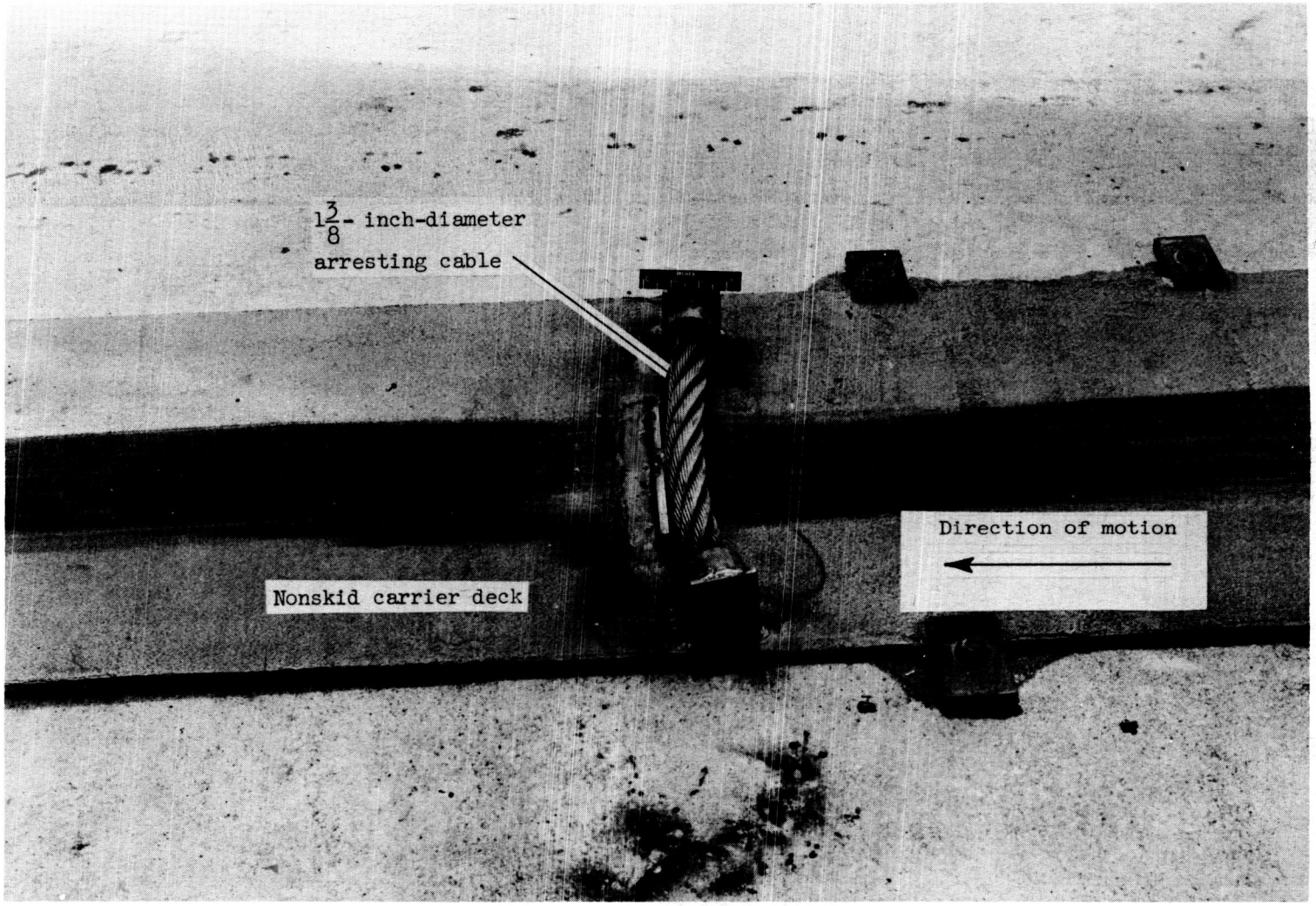

Figure 6.- Arresting cable installation on nonskid carrier deck. L-58-1731.1

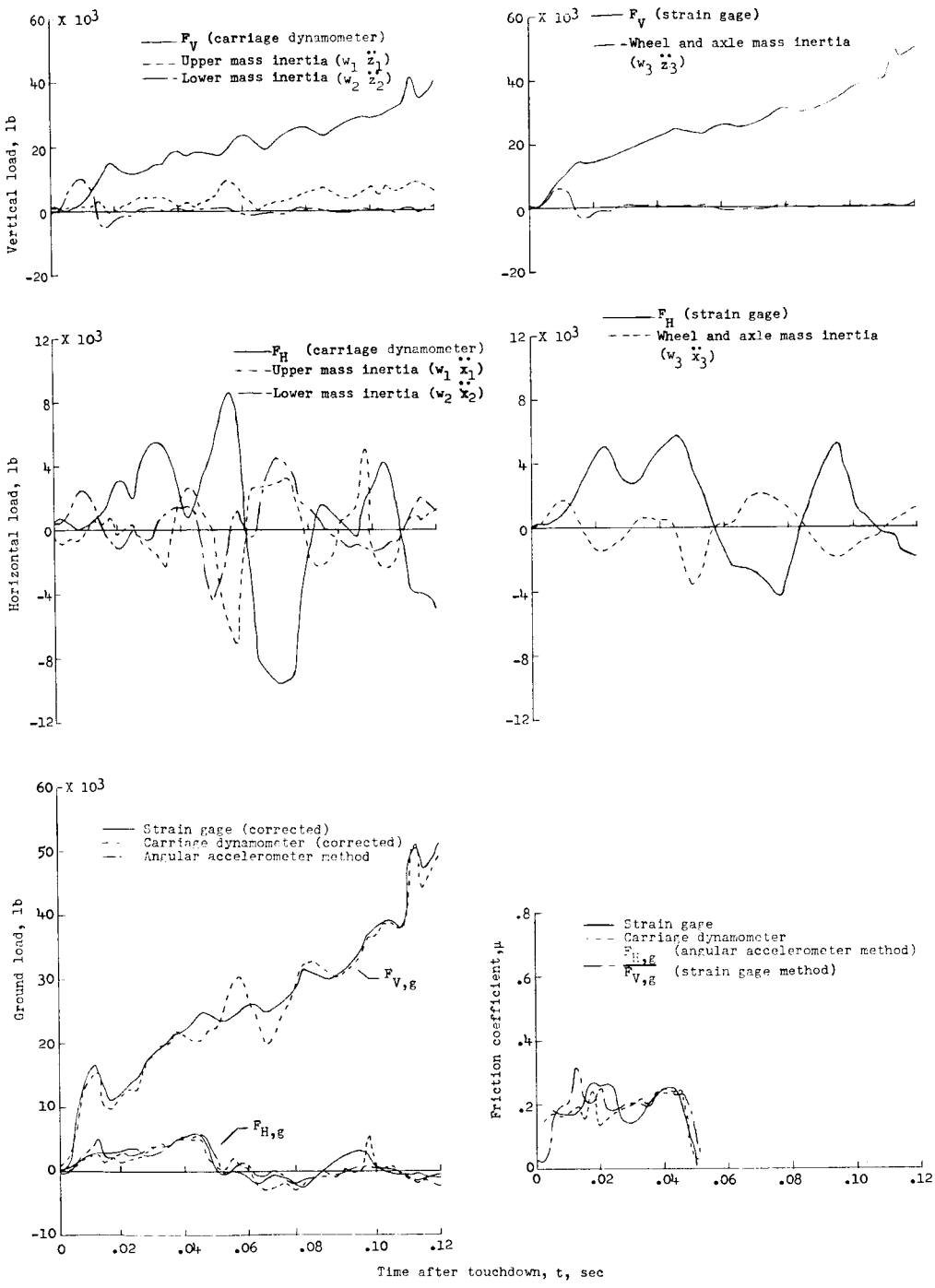

Figure 7.- Typical comparison of simulated landing impact time histories of loads and friction coefficients obtained by the different load measuring methods. Run 30.

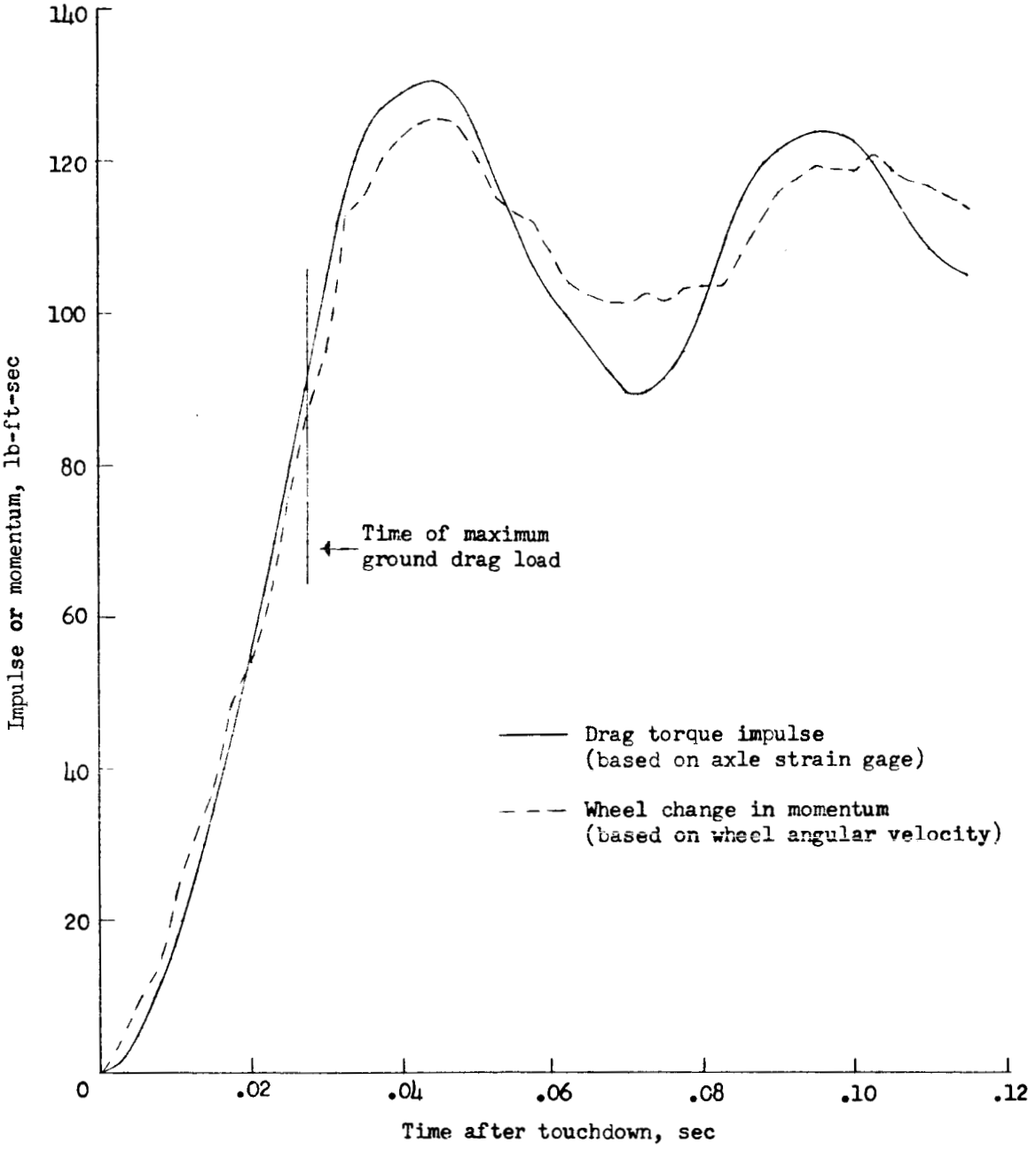

Figure 8.- Typical comparison of the drag torque impulse acting on the wheel during an impact with the resulting change in momentum of the wheel for run 3.

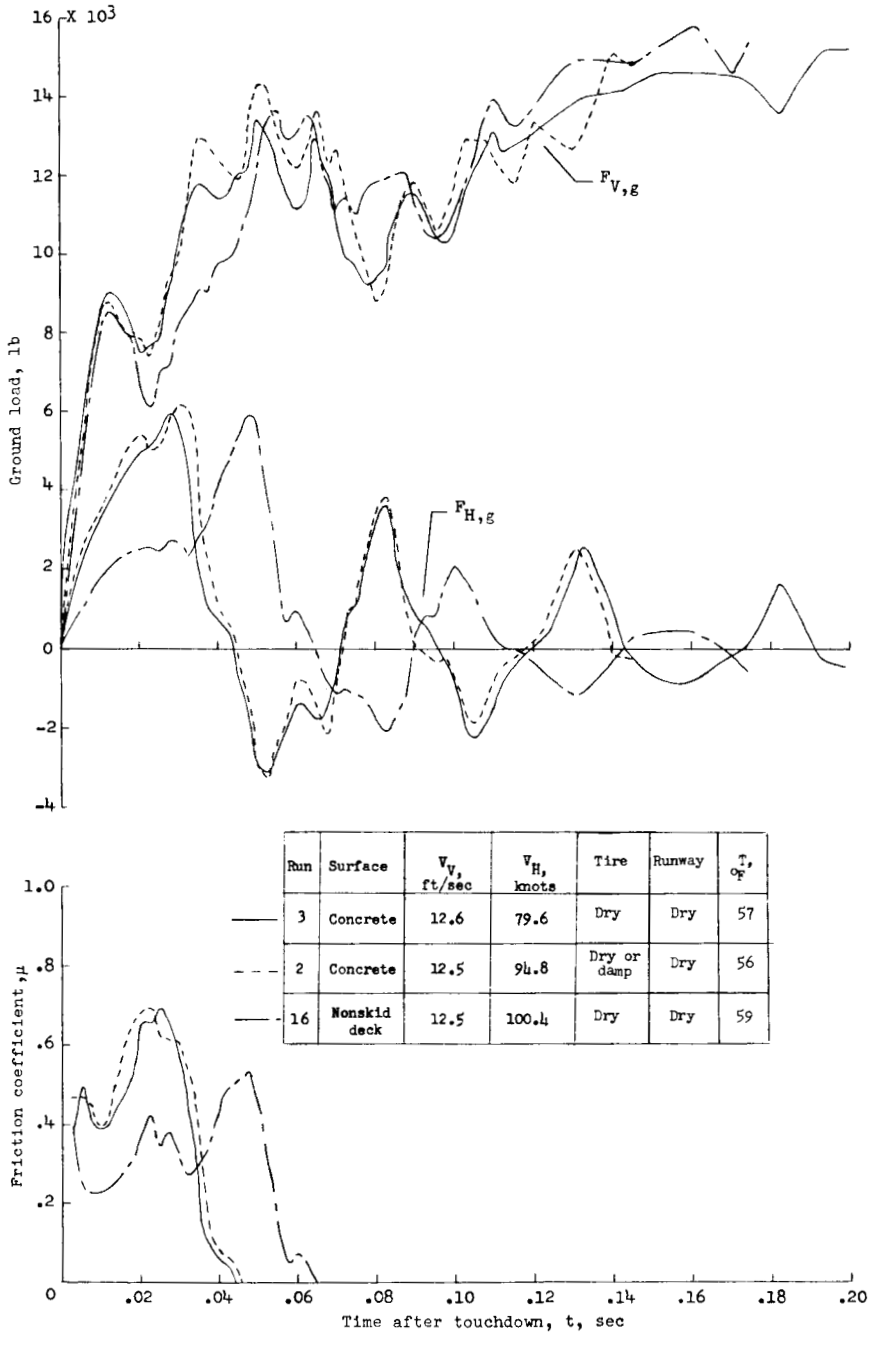

Run	Surface	V_V, ft/sec	V_H, knots	Tire	Runway	T, °F
3	Concrete	12.6	79.6	Dry	Dry	57
2	Concrete	12.5	94.8	Dry or damp	Dry	56
16	Nonskid deck	12.5	100.4	Dry	Dry	59

(a) p_o = 260 pounds per square inch; φ = 2.5° forward.

Figure 9.- Comparison of impacts on concrete and nonskid carrier deck surface for approximately 12 feet per second vertical velocity at touchdown.

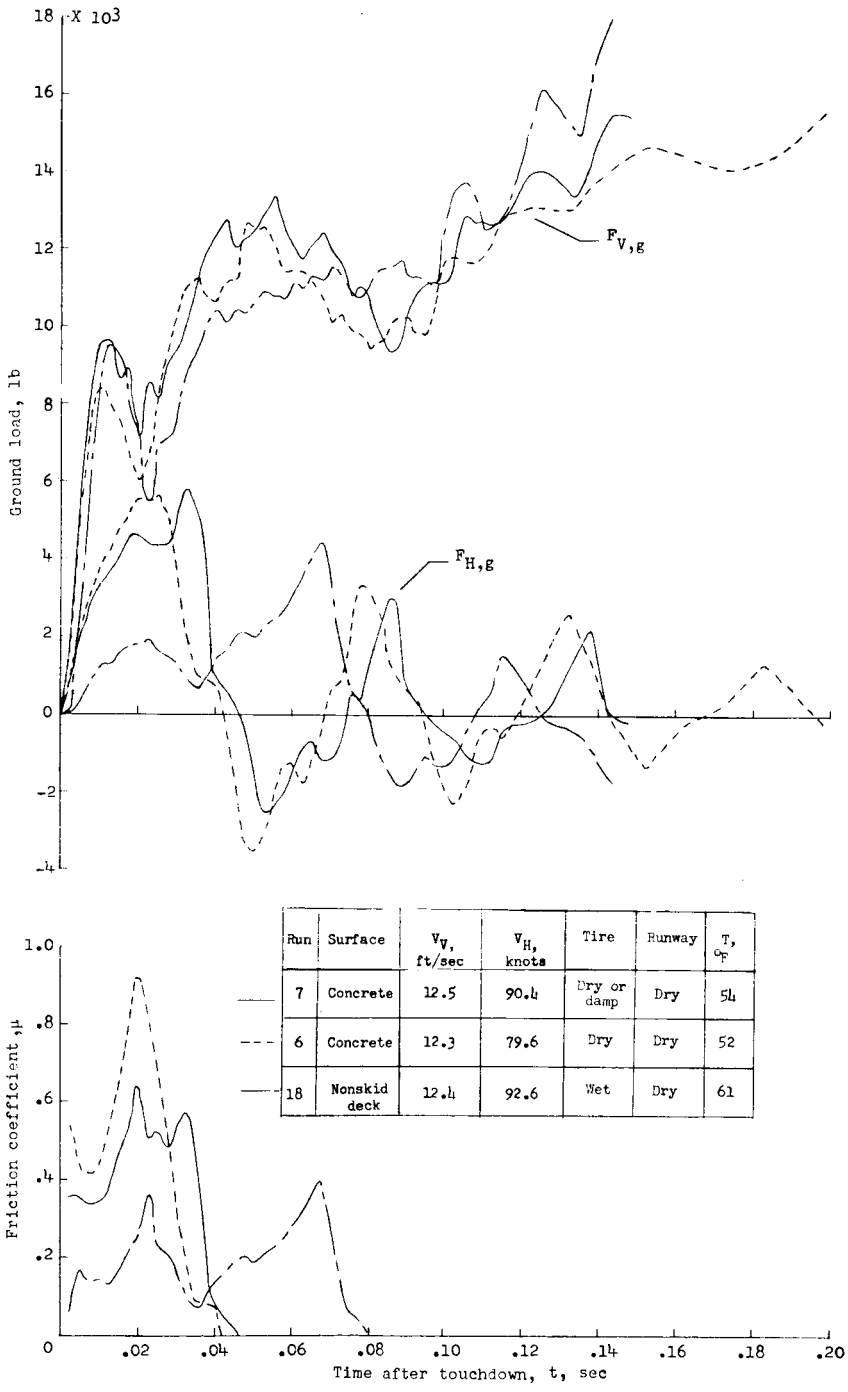

Run	Surface	V_V, ft/sec	V_H, knots	Tire	Runway	T, °F
7	Concrete	12.5	90.4	Dry or damp	Dry	54
6	Concrete	12.3	79.6	Dry	Dry	52
18	Nonskid deck	12.4	92.6	Wet	Dry	61

(b) p_o = 320 pounds per square inch; φ = 2.5° forward.

Figure 9.- Continued.

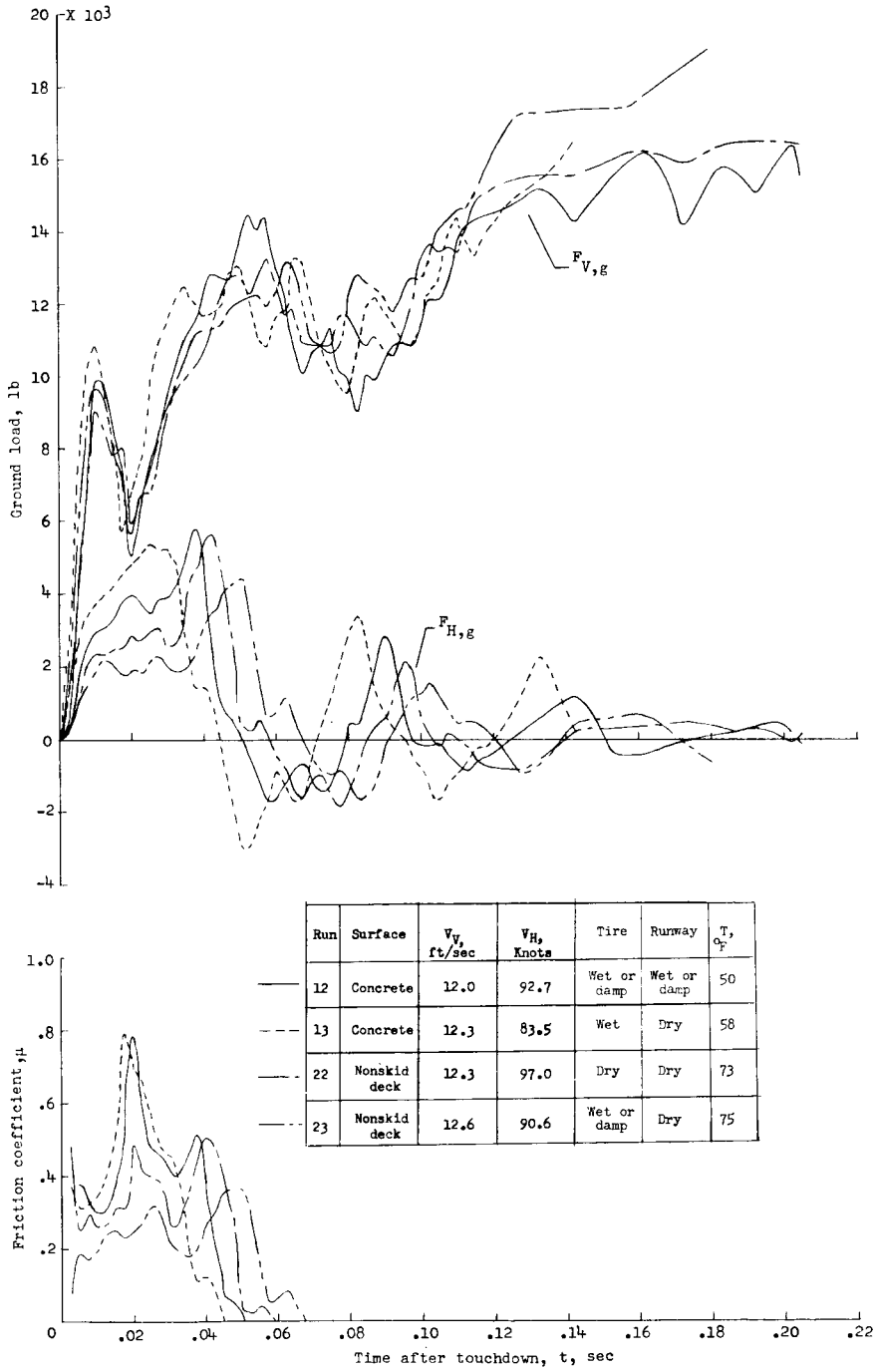

Run	Surface	V_V, ft/sec	V_H, Knots	Tire	Runway	T, °F
12	Concrete	12.0	92.7	Wet or damp	Wet or damp	50
13	Concrete	12.3	83.5	Wet	Dry	58
22	Nonskid deck	12.3	97.0	Dry	Dry	73
23	Nonskid deck	12.6	90.6	Wet or damp	Dry	75

(c) p_o = 400 pounds per square inch; φ = 2.5° forward.

Figure 9.- Concluded.

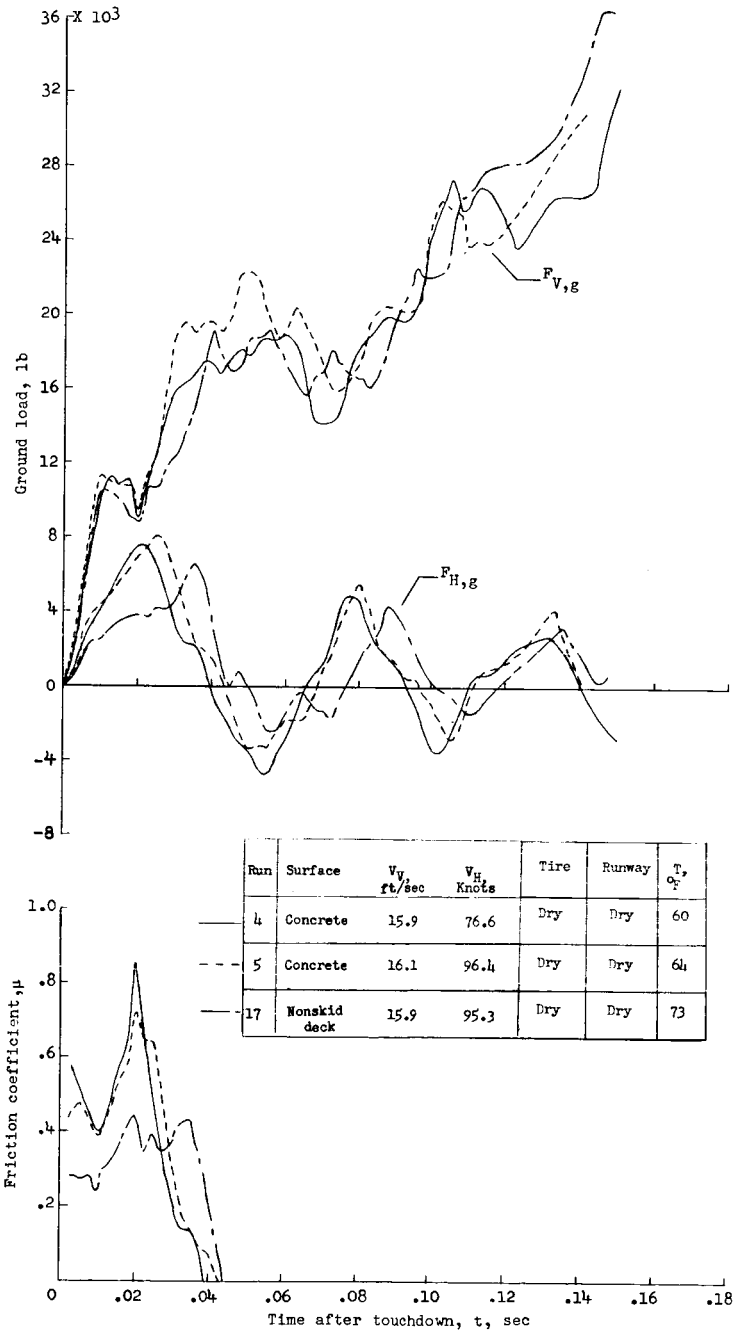

Run	Surface	V_V, ft/sec	V_H, Knots	Tire	Runway	T, °F
4	Concrete	15.9	76.6	Dry	Dry	60
5	Concrete	16.1	96.4	Dry	Dry	64
17	Nonskid deck	15.9	95.3	Dry	Dry	73

(a) p_o = 260 pounds per square inch; φ = 2.5° forward.

Figure 10.- Comparison of impacts on concrete and nonskid carrier deck surface for approximately 16 feet per second vertical velocity at touchdown.

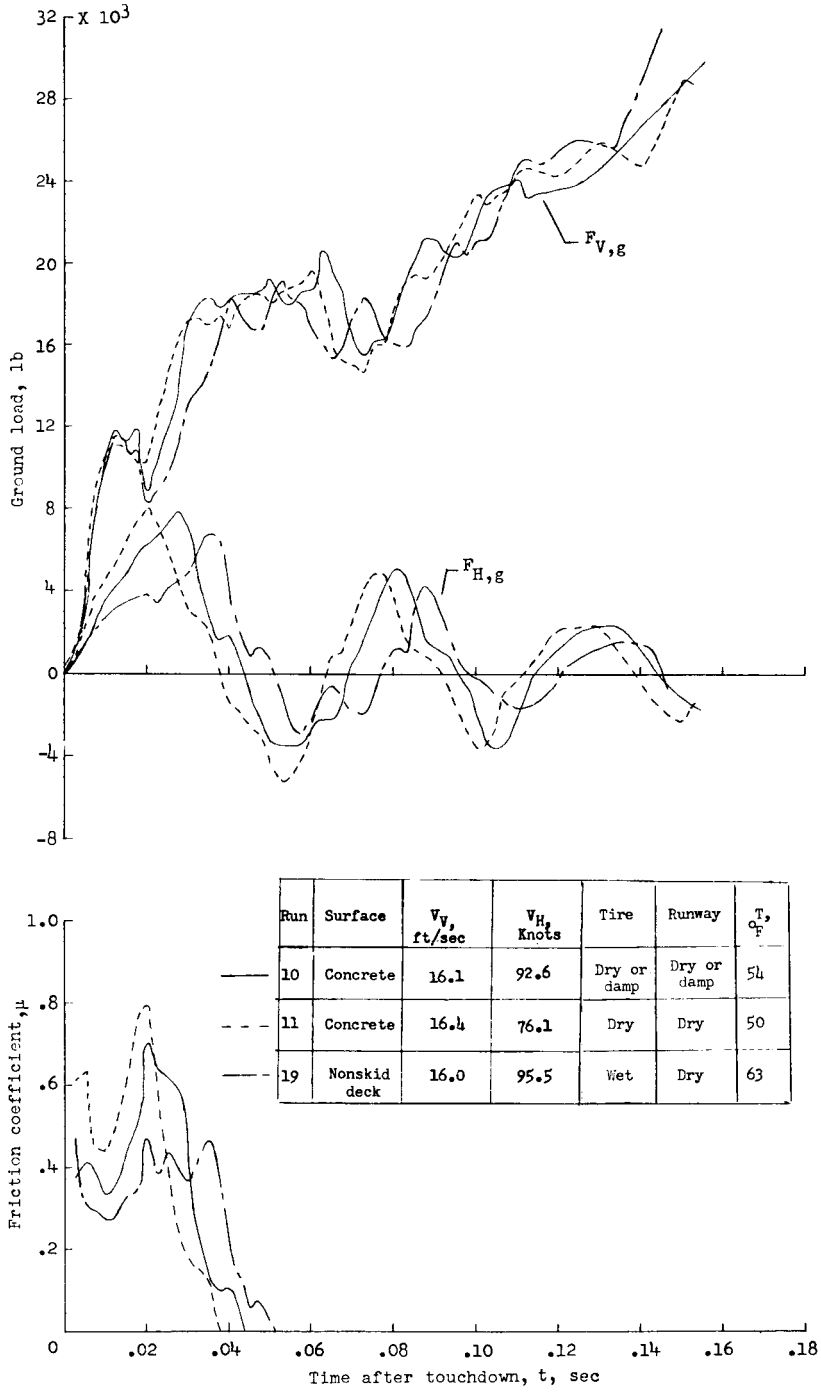

Run	Surface	V_V, ft/sec	V_H, Knots	Tire	Runway	T_F, °F
10	Concrete	16.1	92.6	Dry or damp	Dry or damp	54
11	Concrete	16.4	76.1	Dry	Dry	50
19	Nonskid deck	16.0	95.5	Wet	Dry	63

(b) p_o = 320 pounds per square inch; φ = 2.5° forward.

Figure 10.- Continued.

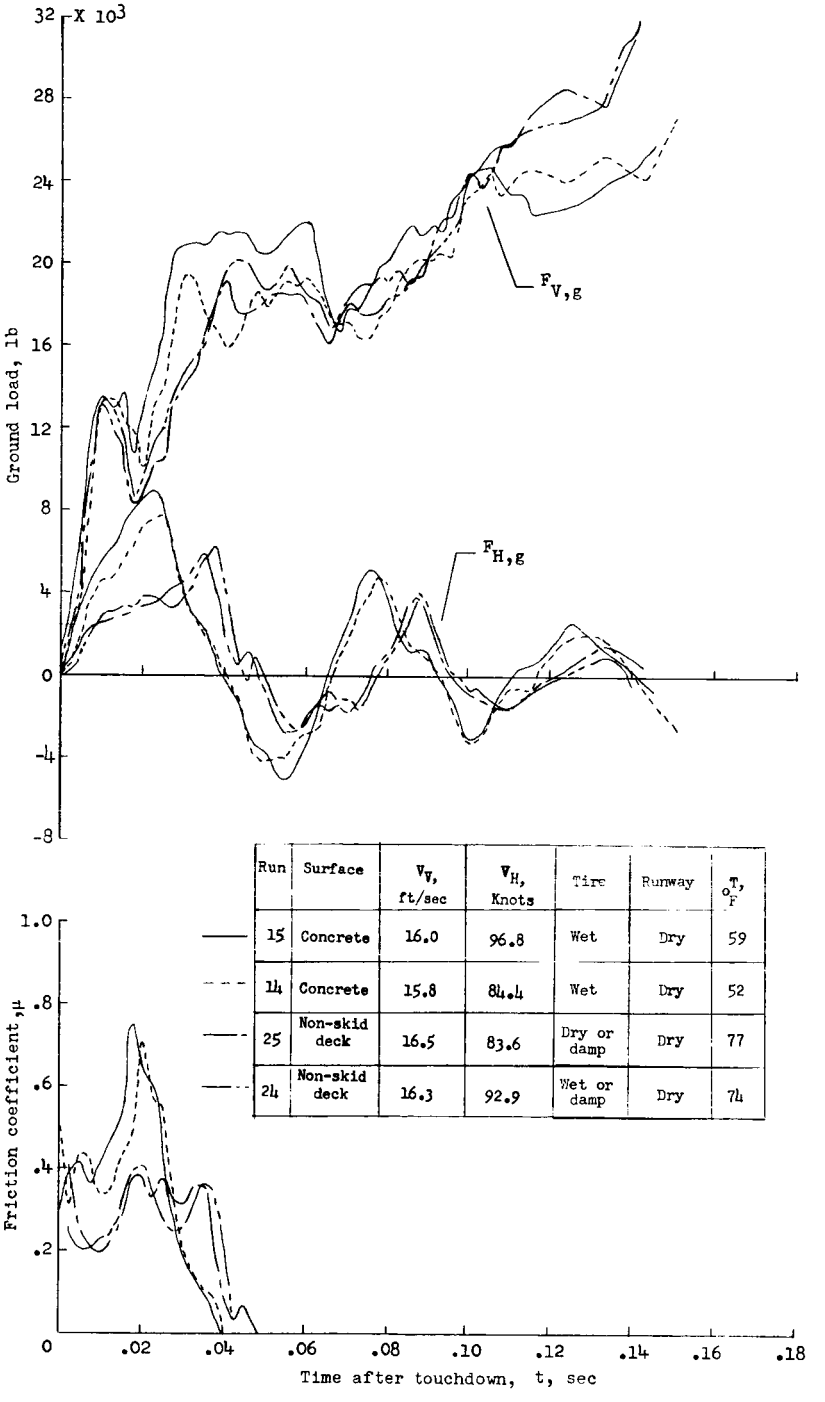

Run	Surface	V_V, ft/sec	V_H, Knots	Tire	Runway	T_o, °F
15	Concrete	16.0	96.8	Wet	Dry	59
14	Concrete	15.8	84.4	Wet	Dry	52
25	Non-skid deck	16.5	83.6	Dry or damp	Dry	77
24	Non-skid deck	16.3	92.9	Wet or damp	Dry	74

(c) p_o = 400 pounds per square inch; φ = 2.5° forward.

Figure 10.- Concluded.

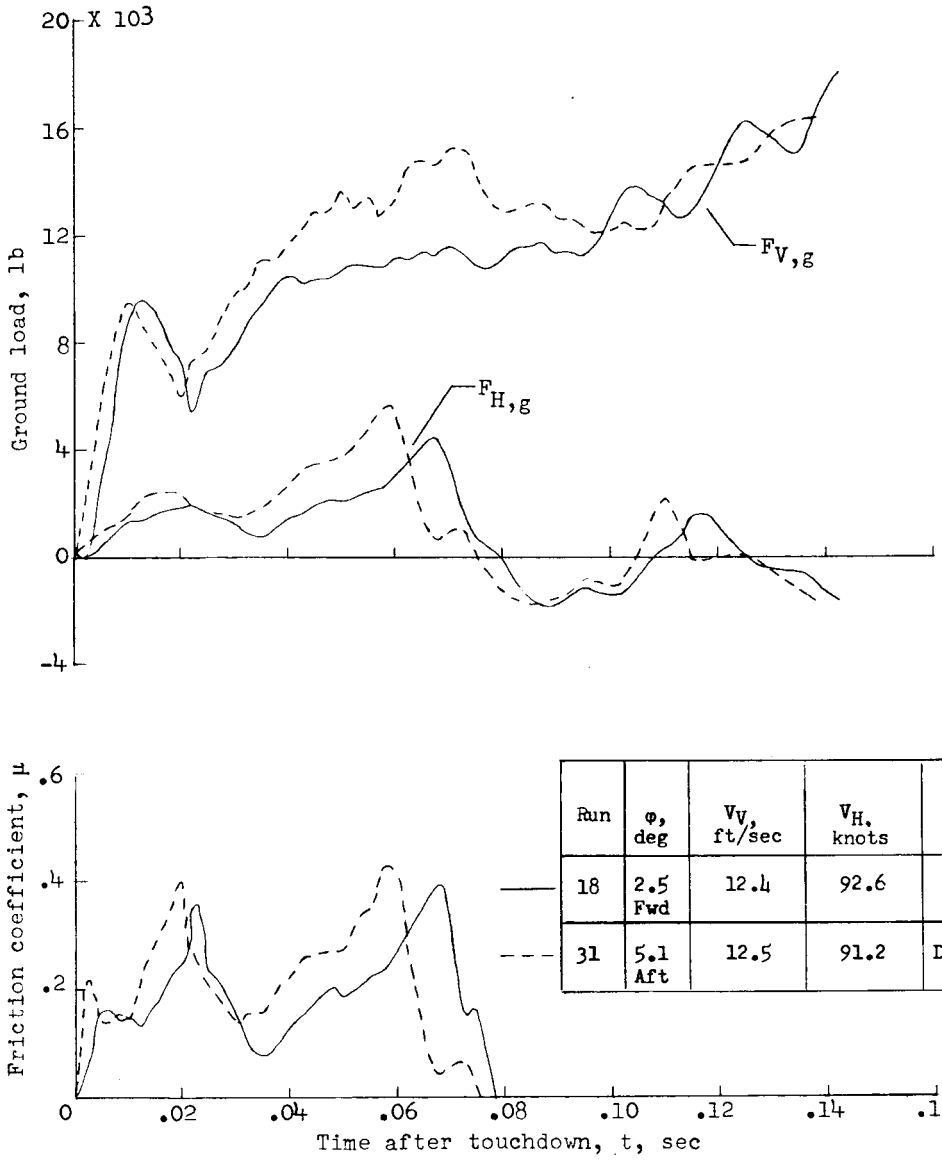

Run	φ, deg	V_V, ft/sec	V_H, knots	Tire	Runway	T, °F
18	2.5 Fwd	12.4	92.6	Wet	Dry	61
31	5.1 Aft	12.5	91.2	Damp or wet	Dry	85

(a) $V_V \approx 12$ feet per second; $V_H \approx 92$ knots.

Figure 11.- Effect of landing-gear inclination on ground load and friction coefficients developed during simulated landings on the nonskid carrier deck. p_o = 320 pounds per square inch.

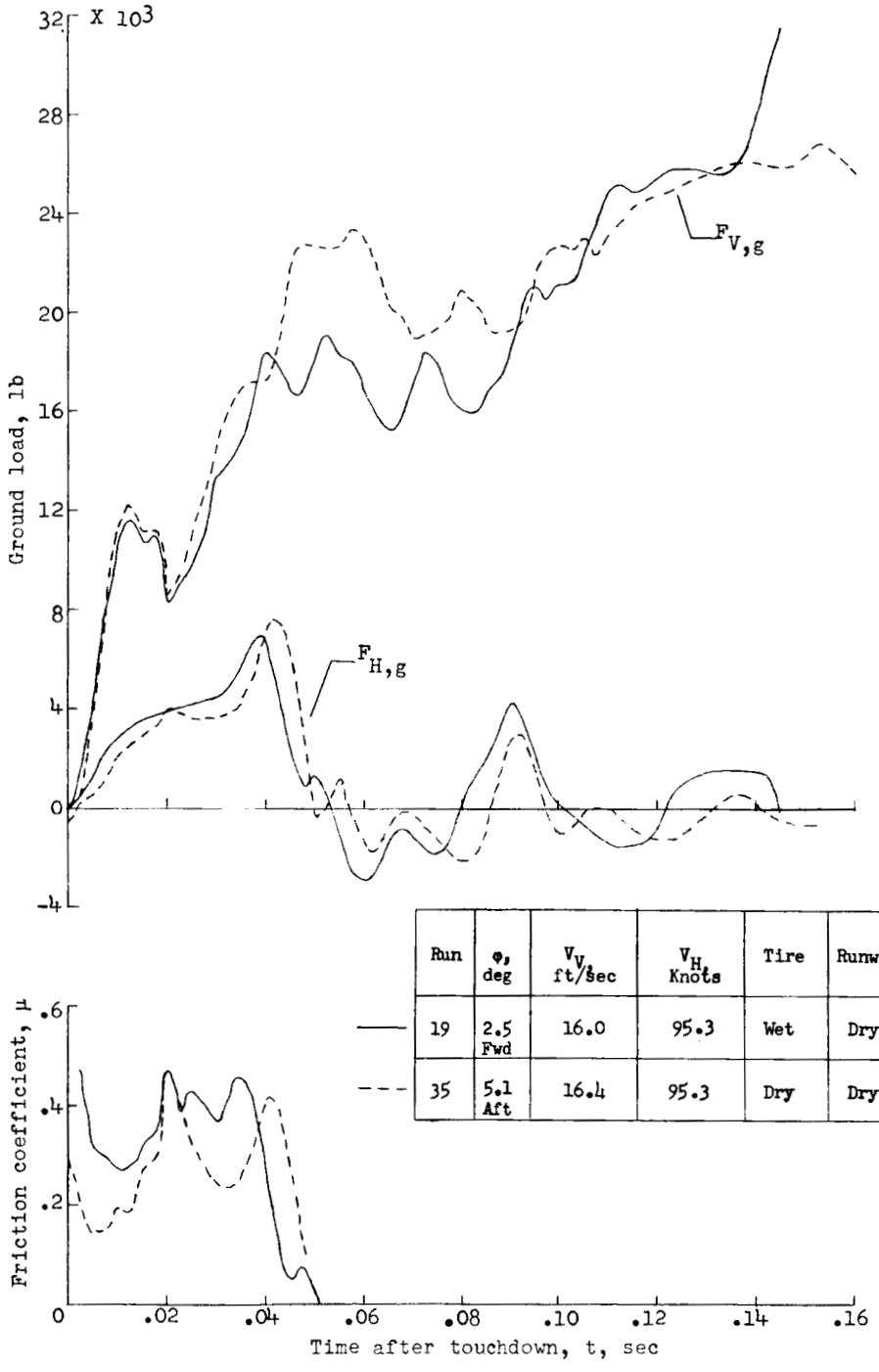

Run	φ, deg	V_V, ft/sec	V_H, Knots	Tire	Runway	T, °F
19	2.5 Fwd	16.0	95.3	Wet	Dry	63
35	5.1 Aft	16.4	95.3	Dry	Dry	85

(b) $V_V \approx 16$ feet per second; $V_H \approx 95$ knots.

Figure 11.- Continued.

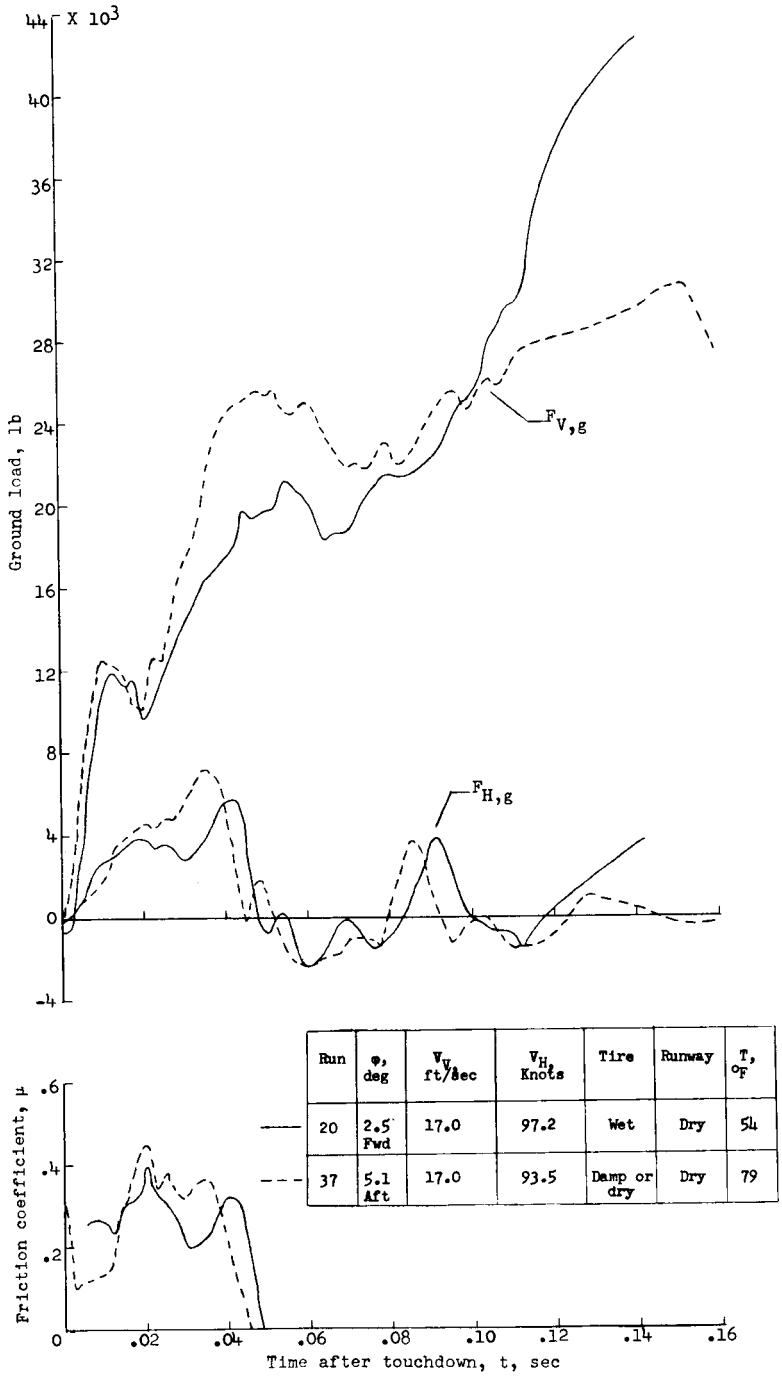

Run	φ, deg	V_V, ft/sec	V_H, Knots	Tire	Runway	T, °F
20	2.5 Fwd	17.0	97.2	Wet	Dry	54
37	5.1 Aft	17.0	93.5	Damp or dry	Dry	79

(c) $V_V \approx 17$ feet per second; $V_H \approx 95$ knots.

Figure 11.- Continued.

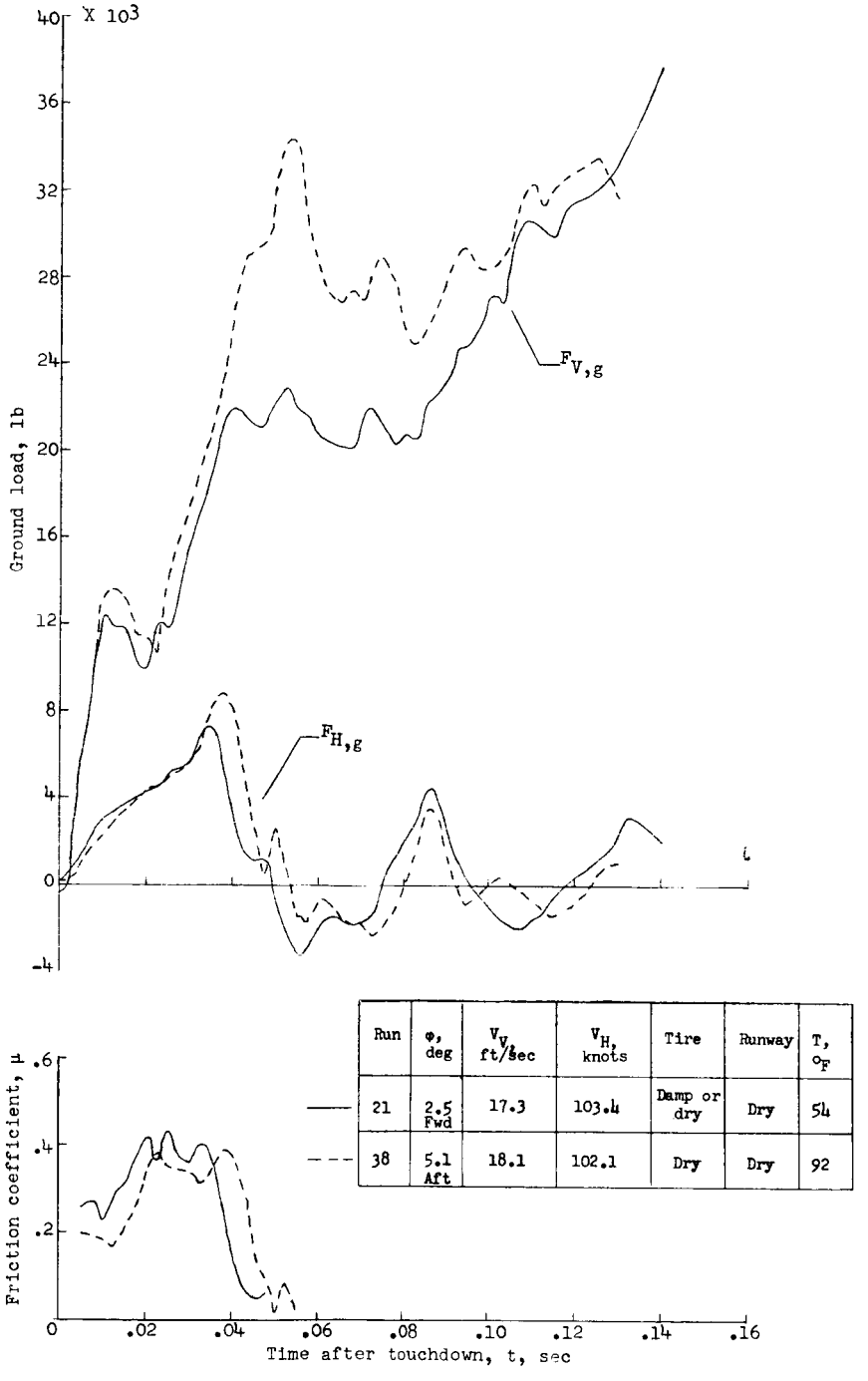

Run	φ, deg	V_V, ft/sec	V_H, knots	Tire	Runway	T, °F
21	2.5 Fwd	17.3	103.4	Damp or dry	Dry	54
38	5.1 Aft	18.1	102.1	Dry	Dry	92

(d) $V_V \approx 18$ feet per second; $V_H \approx 103$ knots.

Figure 11.- Concluded.

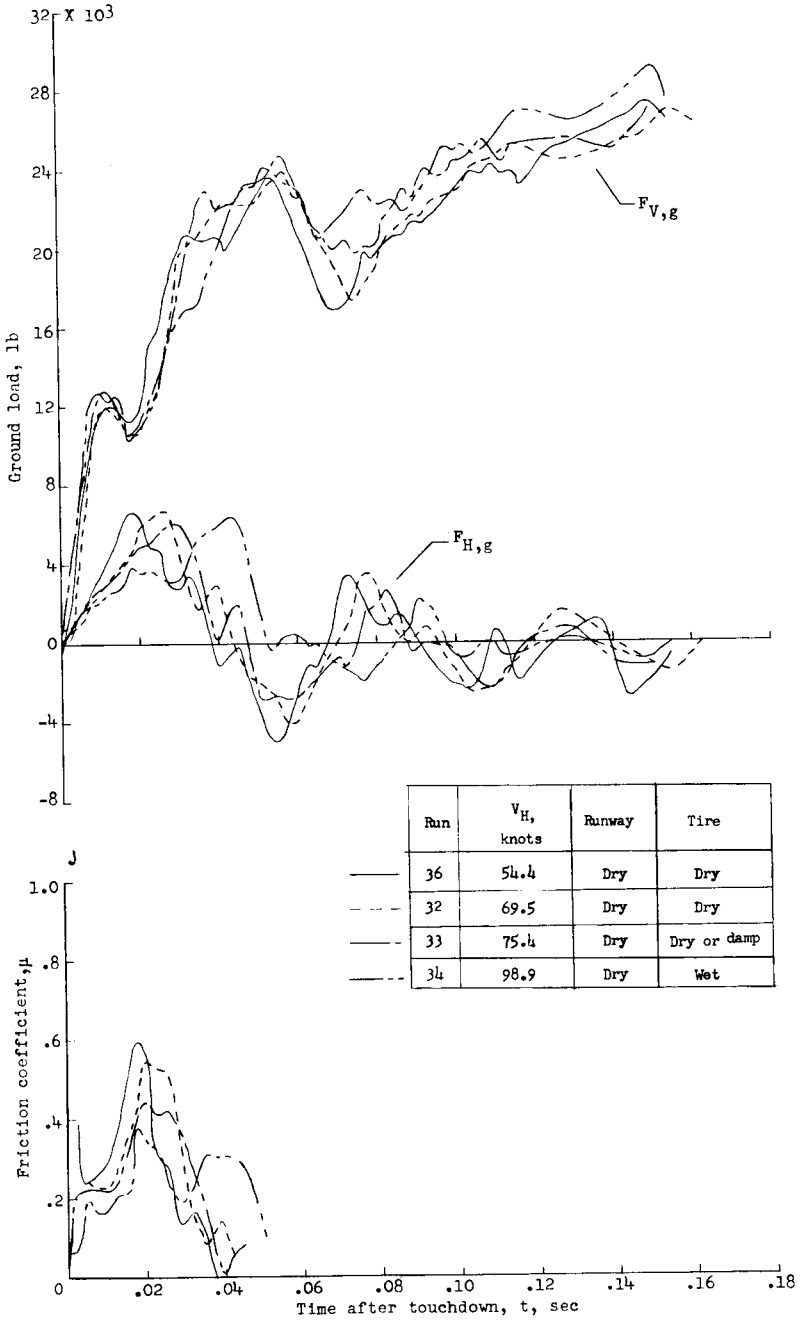

Figure 12.- Effect of forward speed on the ground load and friction coefficients developed during landings on the nonskid carrier deck surface. p_o = 320 pounds per square inch; V_V = 15.6 to 16.4 feet per second; φ = 5.1° rearward.

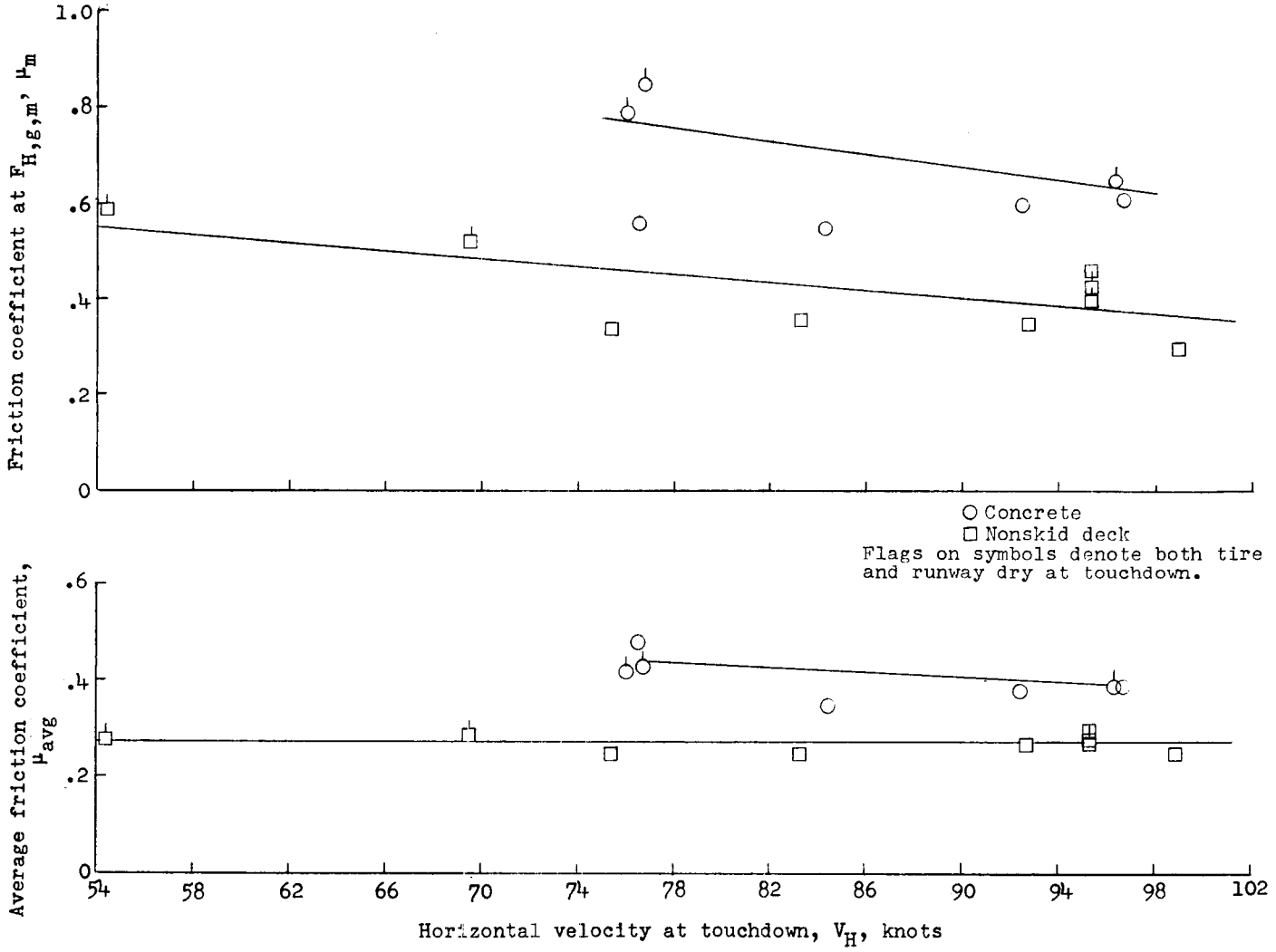

Figure 13.- Effect of forward speed on the spin-up friction coefficients developed on the nonskid deck and concrete surfaces. $V_V \approx 16$ feet per second.

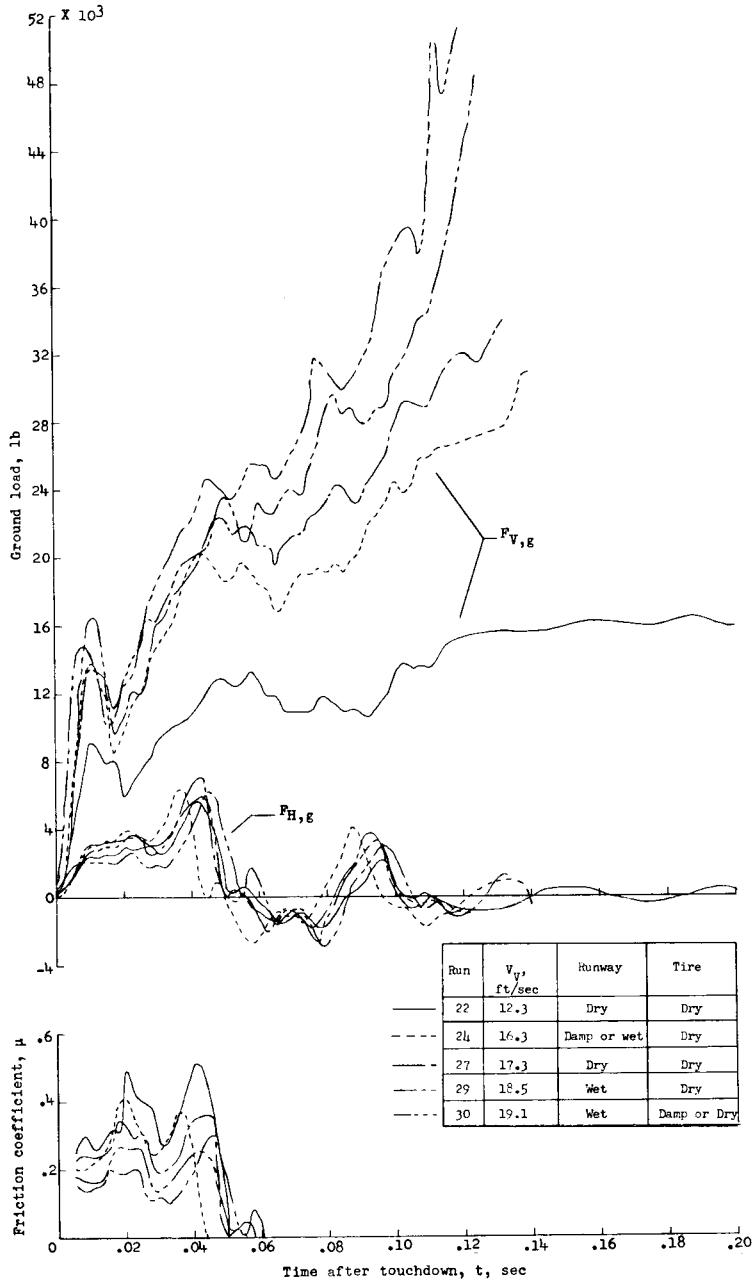

(a) $\varphi = 2.5^{\circ}$ forward.

Figure 14.- Effect of vertical velocity at touchdown on the ground load and friction coefficients developed during landings on the nonskid carrier deck surface. p_o = 400 pounds per square inch; V_H = 86.6 to 104.3 knots.

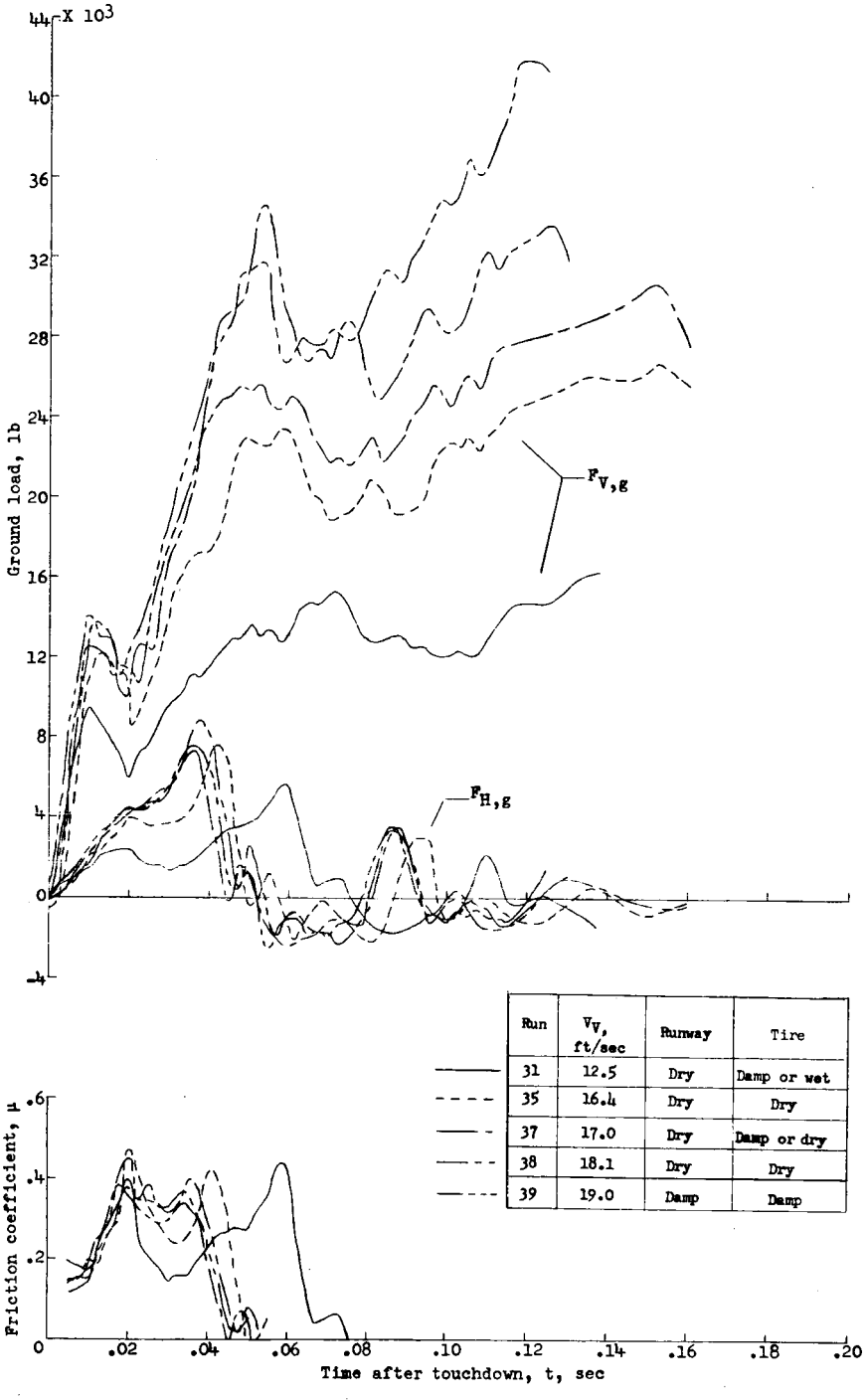

(b) $\varphi = 5.1^{\circ}$ rearward.

Figure 14.- Concluded.

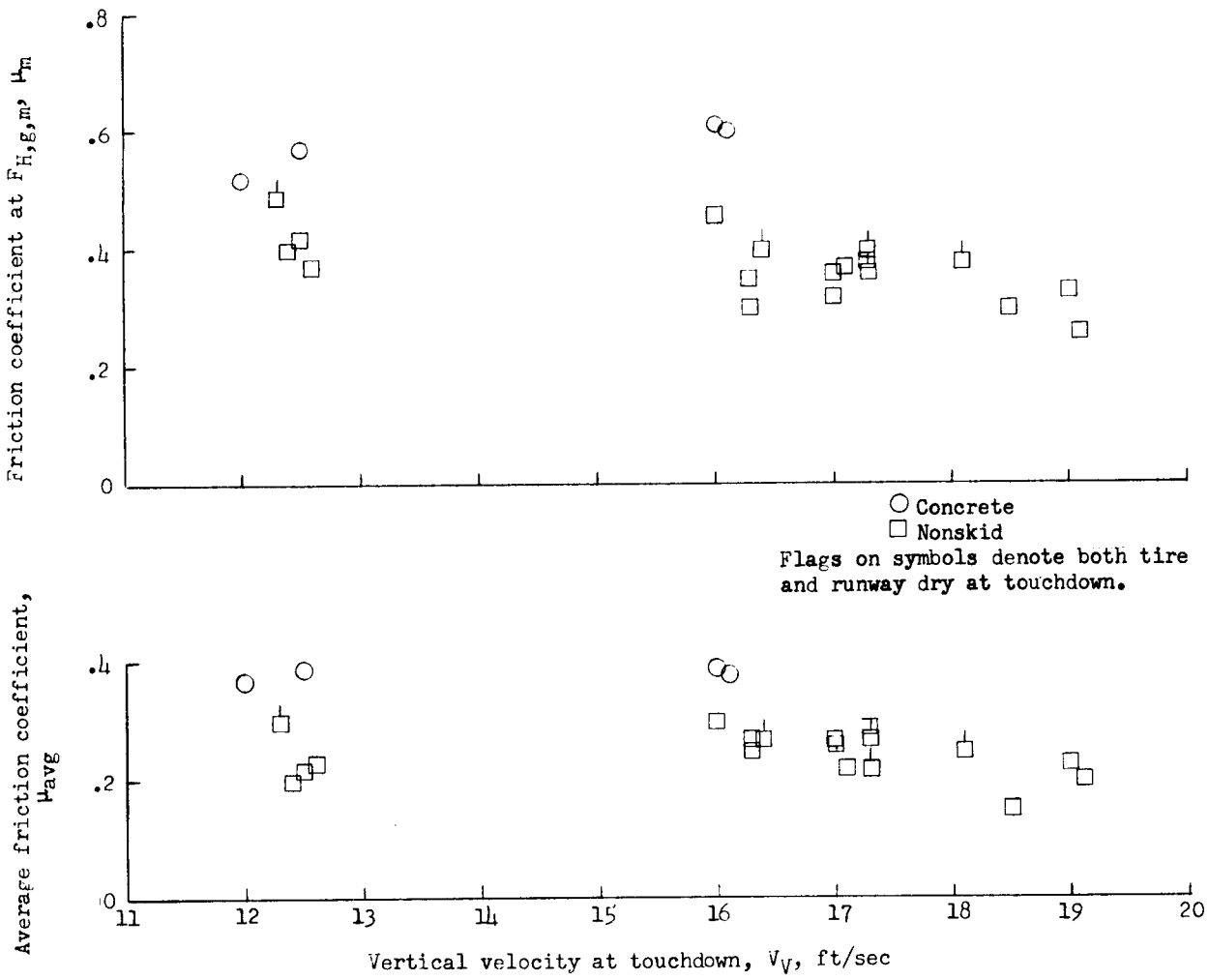

Figure 15.- Effect of vertical velocity on the spin-up friction coefficients developed on the nonskid deck and concrete surfaces. V_H = 85 to 105 knots; p_o = 320 and 400 pounds per square inch.

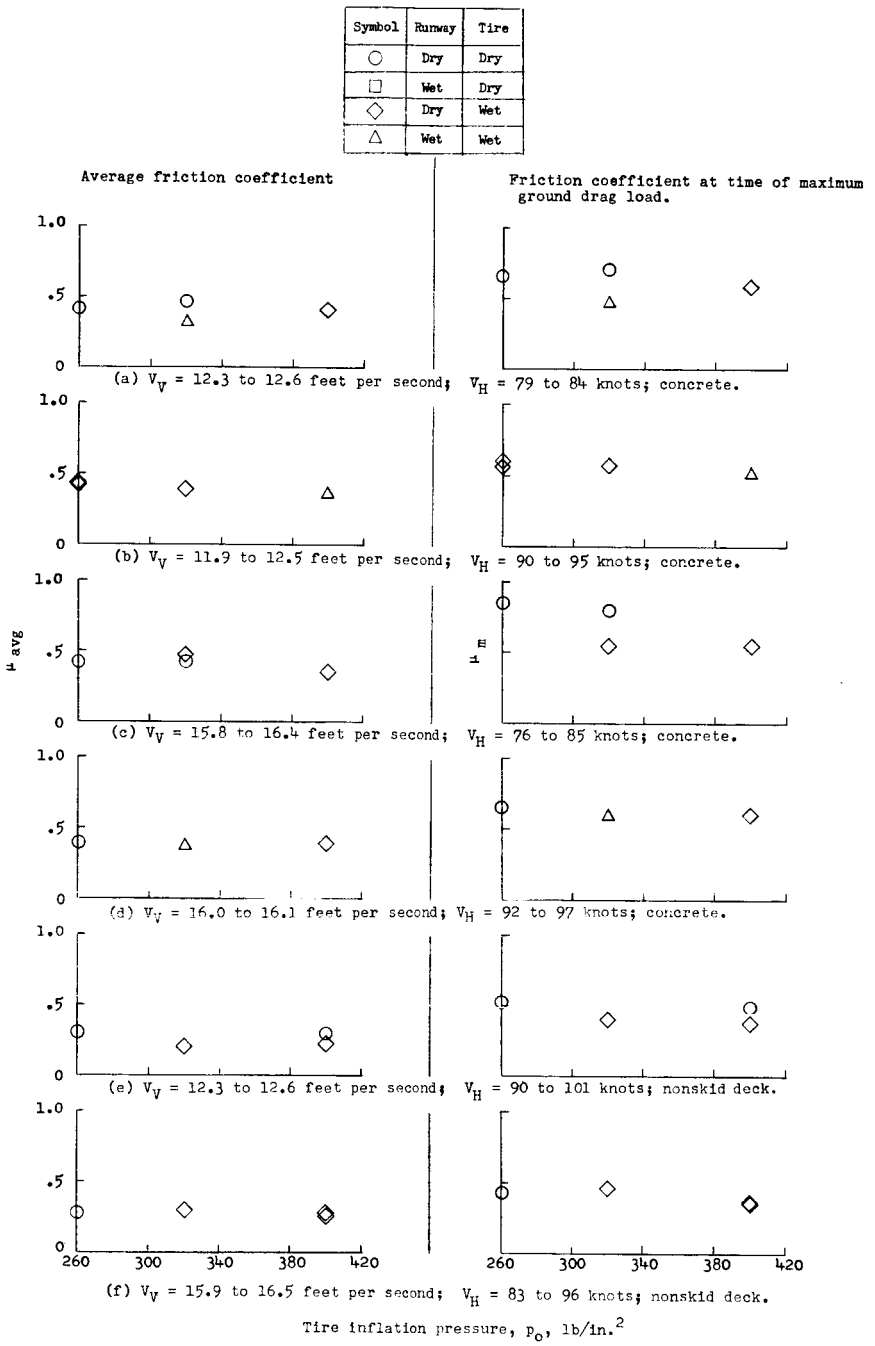

Figure 16.- Effect of tire-inflation pressure on the spin-up friction coefficients developed on the nonskid deck and concrete surfaces. V_V = 12 and 16 feet per second; V_H = 76 to 101 knots; φ = 2.5° forward.

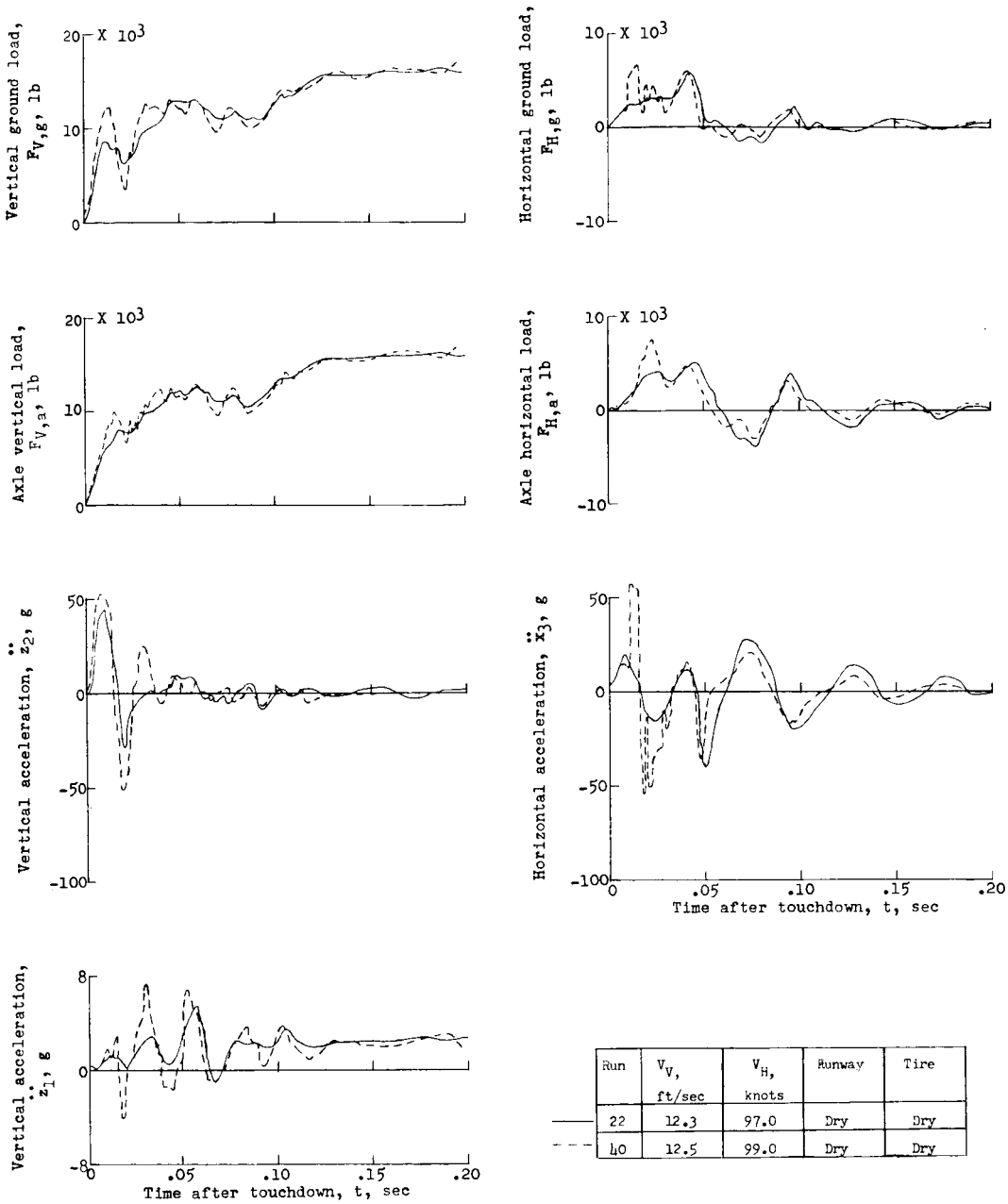

Run	V_V, ft/sec	V_H, knots	Runway	Tire
22	12.3	97.0	Dry	Dry
40	12.5	99.0	Dry	Dry

Figure 17.- Comparison of a 12-feet-per-second sinking-speed impact on the carrier deck surface (run 22) with a similar impact on the $1\frac{3}{8}$-inch-diameter arresting cable (run 40). Impact on the cable occurred before $F_{H,g,max}$; p_o = 400 pounds per square inch; $\varphi = 2.5^\circ$ forward.

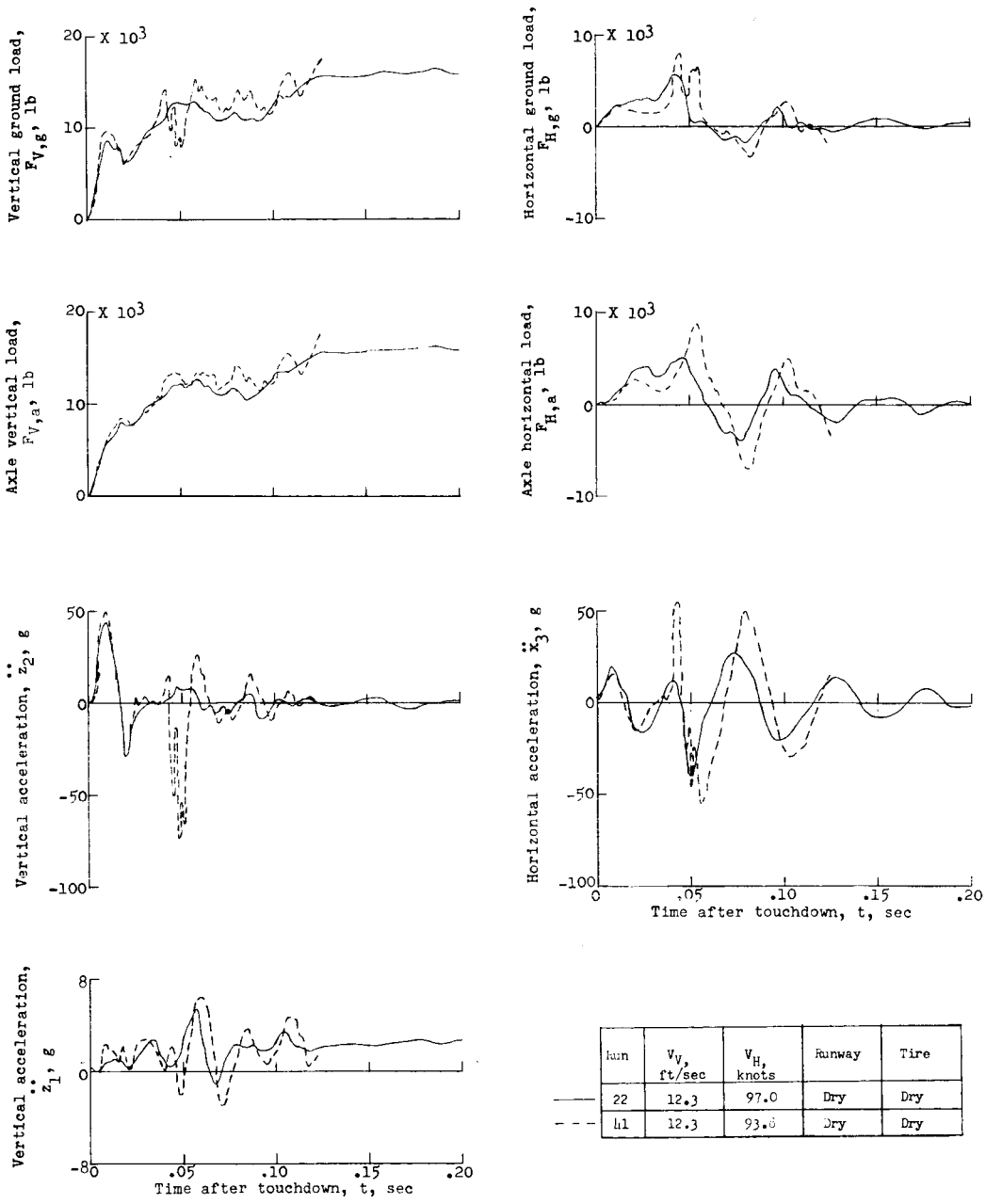

Run	V_V, ft/sec	V_H, knots	Runway	Tire
22	12.3	97.0	Dry	Dry
41	12.3	93.8	Dry	Dry

Figure 18.- Comparison of a 12-feet-per-second sinking-speed impact on the carrier deck surface (run 22) with a similar impact on the $1\frac{3}{8}$-inch-diameter arresting cable (run 41). Impact on the cable occurred at $t = 0.045$ second (at $F_{H,g,max}$); $p_o = 400$ pounds per square inch; $\varphi = 2.5^\circ$ forward.

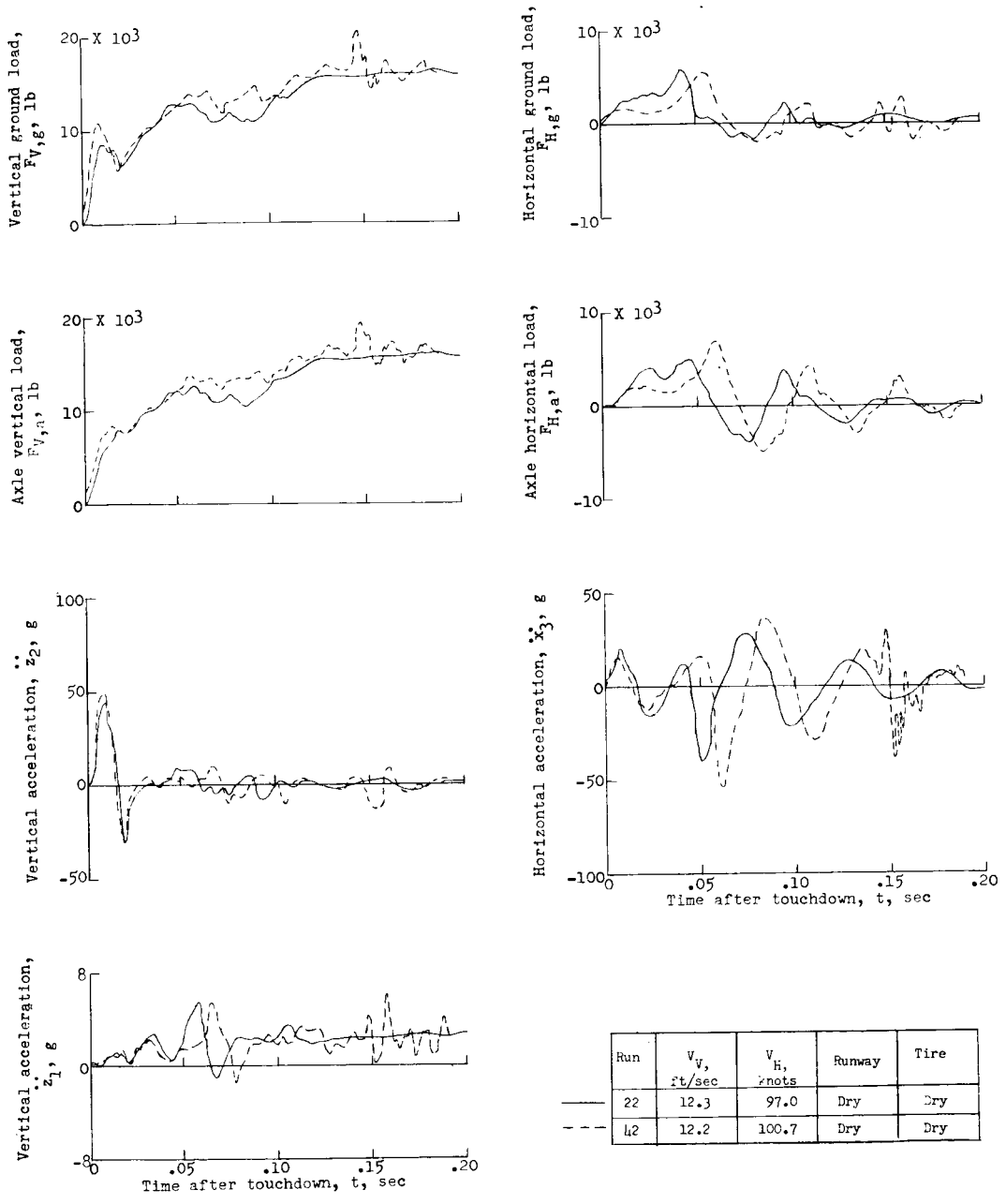

	Run	V_V, ft/sec	V_H, knots	Runway	Tire
——	22	12.3	97.0	Dry	Dry
- - -	42	12.2	100.7	Dry	Dry

Figure 19.- Comparison of a 12-feet-per-second sinking-speed impact on the carrier deck surface (run 22) with a similar impact on the $1\frac{3}{8}$- inch-diameter arresting cable (run 42). Impact on the cable occurred at $t = 0.145$ second $\left(\text{at } F_{V,g,max}\right)$; $p_o = 400$ pounds per square inch; $\varphi = 2.5^\circ$ forward.

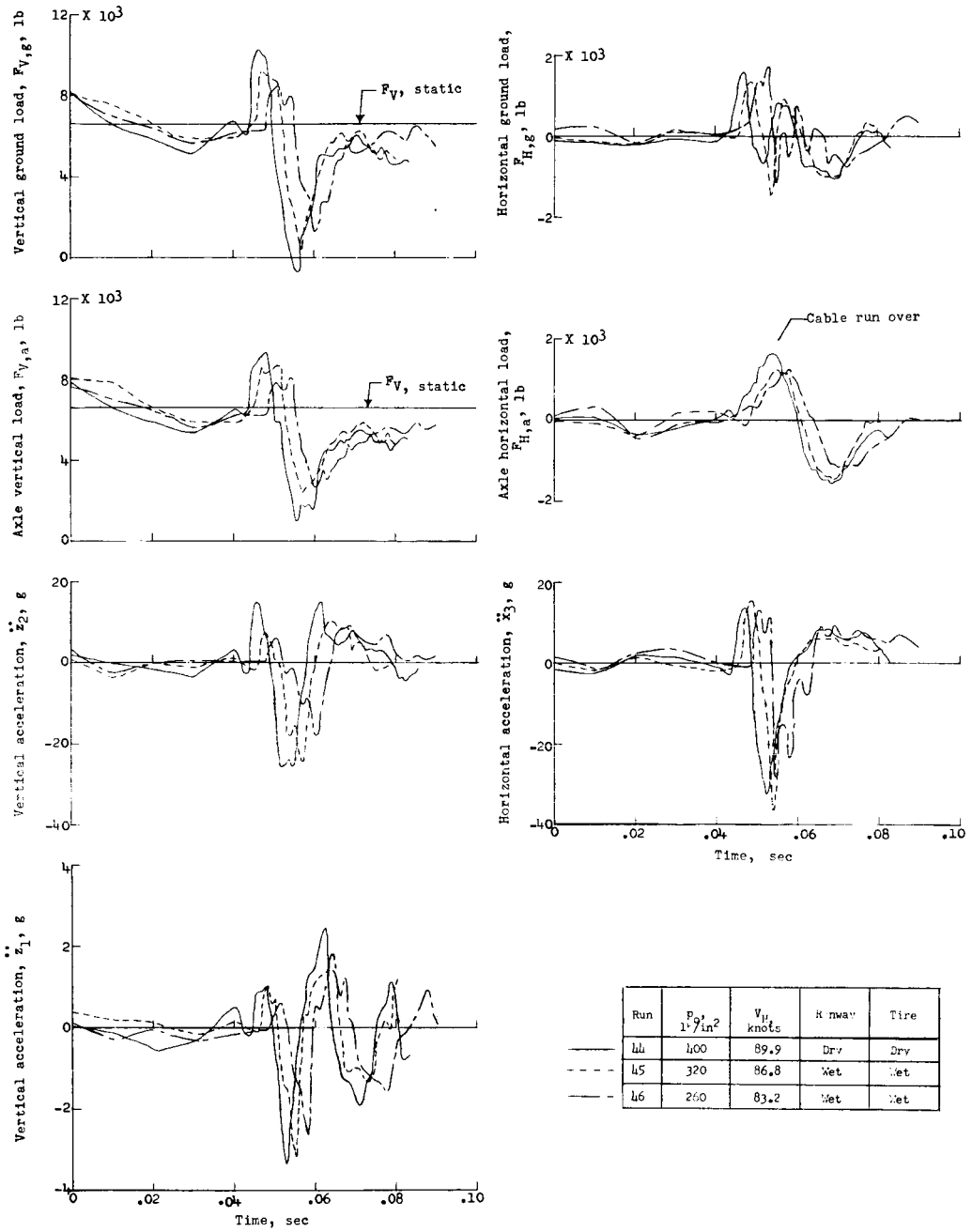

Run	p_g, lb/in²	V_V, knots	Runway	Tire
44	400	89.9	Dry	Dry
45	320	86.8	Wet	Wet
46	260	83.2	Wet	Wet

Figure 20.- Effect of tire-inflation pressure on landing-gear loads and accelerations generated by taxiing over a $1\frac{3}{8}$-inch-diameter arresting cable. $\varphi = 5.1^{\circ}$ rearward; $V_V = 0$; $F_{V,static} = 6{,}630$ pounds; wing lift = 0.

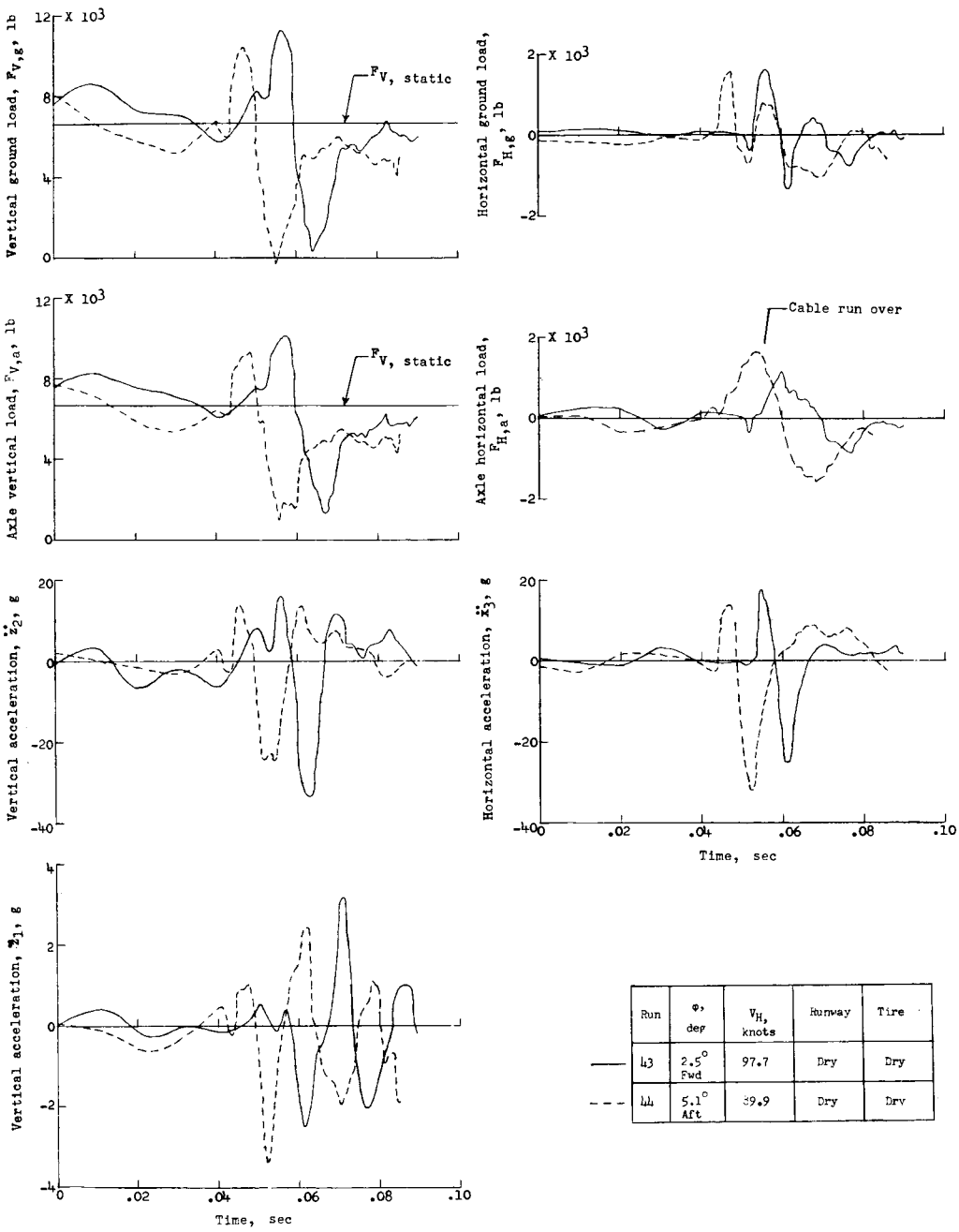

Figure 21.- Effect of shock-strut inclination on landing-gear loads and accelerations generated by taxiing over a $1\frac{3}{8}$-inch-diameter arresting cable. $\varphi = 5.1^\circ$ rearward; $V_V = 0$; $F_{V,static} = 6{,}630$ pounds; wing lift = 0.